Mitochondria-localizing BODIPY-copper(II) conjugates for cellular imaging and photo-activated cytotoxicity forming singlet oxygen

Arnab Bhattacharyya,[a] Aida Jameei,[b] Aditya Garai,[a] Rupak Saha,[a] Anjali A. Karande*[b] and Akhil R. Chakravarty*[a]

[a] Department of Inorganic and Physical Chemistry, Indian Institute of Science and [b] Department of Biochemistry, Indian Institute of Science, Bangalore 560012, India. E-mail: arc@iisc.ac.in; anjali@iisc.ac.in.

Electronic Supplementary Information (ESI)

Table of contents

Experimental section

Methods and measurements:

Elemental analysis (C,H,N) of metal complexes was performed using a Thermo Finnigan FLASH EA 1112 CHNS analyzer. Infrared (IR) and UV-visible absorption studies were done by Bruker Alpha and Perkin-Elmer Spectrum 650 spectrophotometers, respectively, at 25 °C. Emission spectra for ligands and complexes were recorded using a Horiba Jobin-Yvon Fluoromax-4 spectrophotometer. Fluorescence quantum yield determination was done with respect to fluorescein as standard following literature procedures.[1] For Electrospray ionization (ESI) mass spectral analysis, Agilent 6538 Ultra high definition (UHD) accurate Mass-Q-TOF (LC-HRMS) and Bruker Daltonics make Esquire 300 Plus ESI model mass spectrometers were used. Bruker Avance 400 NMR spectrometer (400 MHz) was helpful to record the NMR spectra of all samples. FACS analysis (flow cytometry) was performed using FACS Calibur (Becton Dickinson (BD) cell analyzer) and Confocal microscopic experiments were done using Leica TCS (SP5 DM6000) laser scanning confocal microscope at 63X magnification.

Cyclic voltammetric experiments

Cyclic voltammetric studies were performed at 25 °C on an EG&G PAR model 253 VersaStat potentiostat/galvanostat with electrochemical analysis software 270. The three electrode setup used for the studies consist glassy carbon as working, platinum wire as auxiliary and saturated calomel (SCE) as the reference electrode. DMF was used as solvent and tetrabutylammonium perchlorate (TBAP) (0.1 M) was used as supporting electrolyte while ferrocene was the standard compound taken for all studies. The complexes showed one-electron quasi-reversible redox process near –0.1 V in DMF-0.1 M TBAP corresponding to the Cu(II)-Cu(I) couple. The BODIPY complex **2** in addition displayed a quasi-reversible wave near –1.1 V assignable to the reduction of the borondipyrromethene component of L^2. Same process was observed at –0.85 V in the diiodoBODIPY complex **3**. The redox activity at near zero potential could result some “chemical nuclease” activity in presence of cellular thiols.

DNA binding and cleavage experiments

DNA binding: DNA binding experiments were done for complexes 1-3 in Tris-HCl buffer (pH, 7.2) and PBS buffer. Calf Thymus (ct) DNA was used as DNA source. For the determination of intrinsic equilibrium binding constant (K_b) values, UV−visible absorption titration experiments were helpful where each of the complexes **1-3** (40 μM) taken in 5 mM Tris-HCl buffer (pH = 7.2) containing 5% DMF was titrated gradually against 190 μM of ct-DNA (10 μL addition each time) and the change in absorbance was monitored at the respective absorption maxima. McGhee−von Hippel (MvH) method using the expression of Bard and co-workers were used for the calculations.[2,3]

DNA cleavage: Supercoiled pUC19 DNA (30 μM, 0.2 μg, 2686 base-pairs) cleavage was monitored using electrophoresis in agarose gel with the copper(II) complexes in a 50 mM tris-(hydroxymethyl)methane-HCl (Tris-HCl) buffer (pH 7.2) containing 50 mM NaCl. To monitor chemical nuclease activities, complexes 1-3 of 10 μM (2 μL) was incubated with DNA (1 μL) in presence of glutathione (4 μL, 500 μM), NaCl/Tris-HCl buffer (12 μL) and kept in the dark for 1 h at 37° C. The samples after incubation were added to the loading buffer (0.25% bromophenol blue, 0.25% xylene cyanol, 30% glycerol, 3 μL) and then loaded on 1% agarose gel containing 1.0 μg/mL ethidium bromide. Electrophoresis was then carried out in a dark chamber for 2 h at 65 V in TAE (Tris-acetate EDTA) buffer (pH ~ 8.5). For DNA photo cleavage studies, the reactions were carried out in visible light of 532 nm wavelength using a Spectra Physics laser (CW, beam diameter 0.32±0.02 mm, power = 100 mW) following standard protocols.[4] After light exposure, each sample was incubated for 1.0 h at 37° C and analyzed for the photocleaved products using agarose gel electrophoresis. For mechanistic studies, different additives as quenchers of singlet oxygen (NaN_3, 4 mM; TEMP, 4 mM) and scavengers of hydroxyl radicals (DMSO, 4 μL; KI, 4 mM; catalase, 4 units) were used. Superoxide dismutase (4 units) was used as a scavenger of $O2^{\bullet-}$ radicals. The concentrations of the complexes and additives corresponded to that in the 20 μL final volume of the sample using Tris buffer. The errors of calculation were in between 3−5% with respect to the band intensities.

Singlet oxygen quantum yield determination studies:

Quantification of singlet-oxygen generation: Singlet-oxygen-generation experiments were performed with a Spectra Physics CW laser of 532 nm having power of 100 mW. Throughout the experiment, intensity of the laser beam was kept constant. Singlet oxygen Quantum yields (in DMSO) were calculated by recording the change in UV-Vis absorption maxima of DPBF in presence of complex **3** and ROSE Bengal (RB). DPBF is used as convenient acceptor because it of its ability not only to absorb in a region of dye-transparency but also due to its potential for rapid scavenging of singlet oxygen to produce colourless products. This reaction happens with little-or-no physical quenching. All UV-vis spectra were taken at low dye concentrations (optical density: 0.12–0.15 at irradiation wavelengths >530 nm) to minimize the possibility of singlet-oxygen quenching by the dyes. In each measurement, the photooxidation of DPBF was monitored between the 5 sec to 40 sec. No thermal recovery of DPBF (from a possible decomposition of the endoperoxide product) was observed under these experimental conditions. The quantum yields of singlet oxygen generation ($\Phi[^1O_2]$ or Φ_Δ) were calculated using indirect method by comparing the quantum yield of the photooxidation of DPBF that was sensitized by the compound of interest to the quantum yield of Rose Bengal (RB) (Φ_Δ = 0.76 in DMSO) as a reference compound according to Equation (1), where subscripts "c" and "RB" denote complex **3** and Rose Bengal, respectively, Φ_Δ is the quantum yield of singlet oxygen, "m" is the slope of a plot with a difference in the change in the absorbance of DPBF (at 417 nm) with the irradiation time, and "F" is the absorption correction factor, which is given by $F=1–10^{-OD}$, where OD is the optical density at the irradiation wavelength.

$$\Phi\Delta_c = \Phi\Delta_{RB} \times (m_c/m_{RB}) \times (F_{RB}/F_c) \qquad \text{---- eq. (1)}$$

References:

1. J. Q. Umberger and V. K. Lamer, *J. Am. Chem. Soc.*, 1945, **67**, 1099–1109.

2. J. D. McGhee and P. H. Von Hippel, *J. Mol. Biol.*, 1974, **86**, 469–489.

3. M. T Carter, M. Rodriguez and A. J. Bard, *J. Am. Chem. Soc.*, 1989, **111**, 8901–8911.

4. (a) F. M Ausubel, R. Brent, R. E Kingston, D. D Moore, J. G Seidman, J. A Smith and K. Struhl, *Cur. Protocols in Mol. Biol.*, John Wiley & Sons: New York, 2003; (b) J. Bernadou, G. Pratviel, F. Bennis, M. Girardet and B. Meunier, *Biochemistry*, 1989, **28**, 7268–7275.

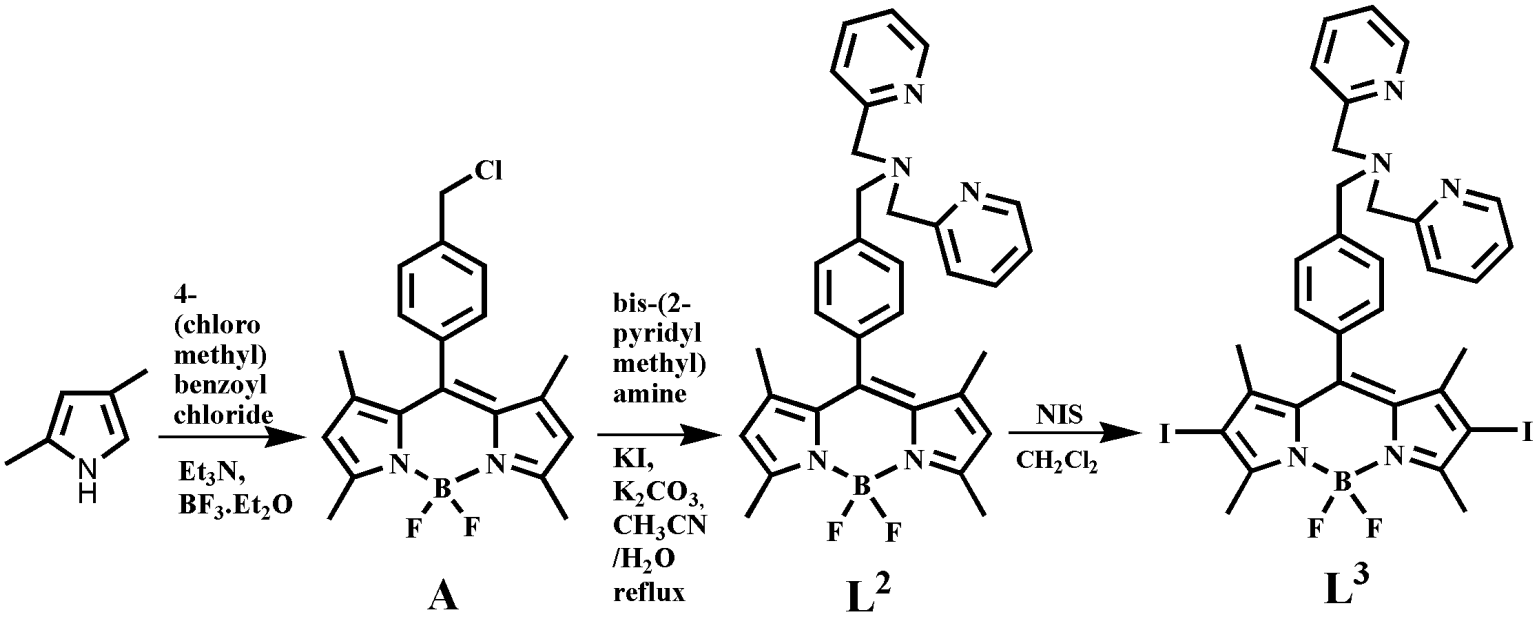

Scheme 1. Synthetic process for the BODIPY ligands (L^2 and L^3).

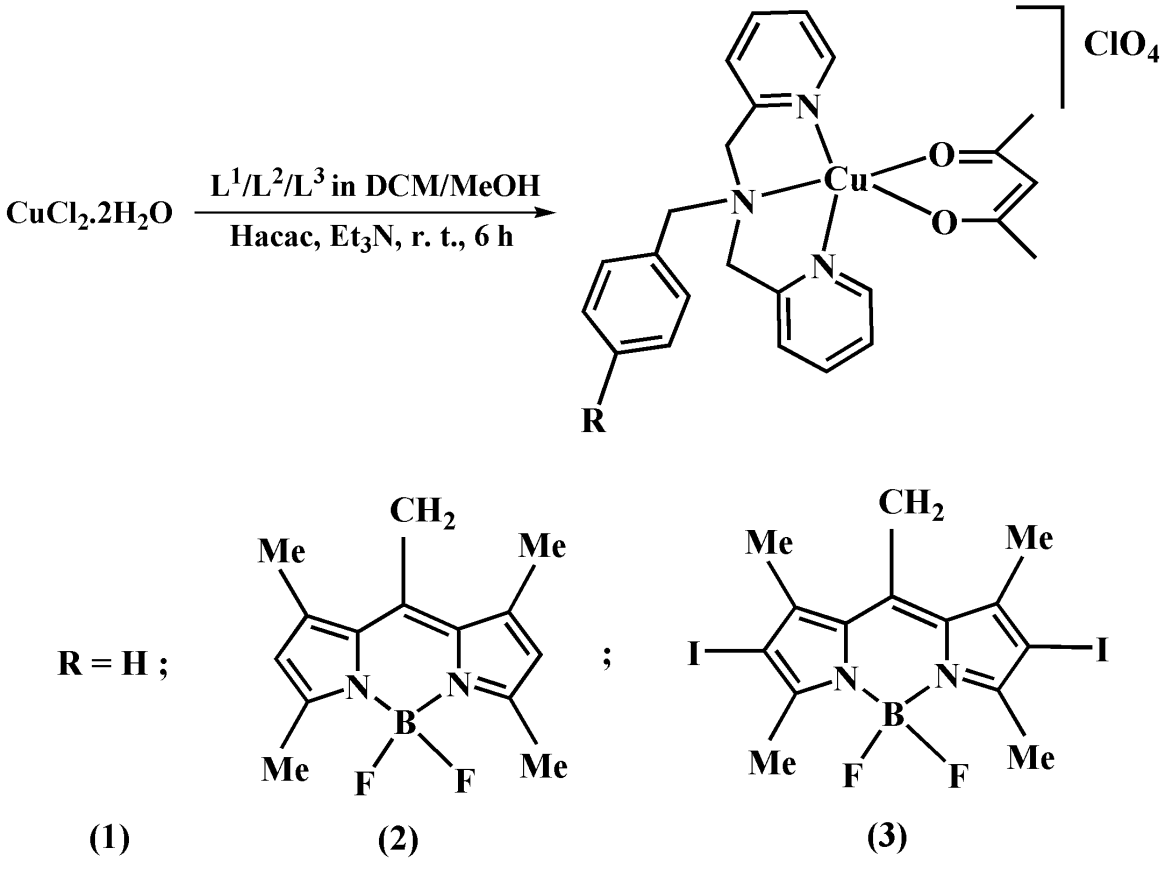

Scheme 2. Synthesis of complexes **1-3**.

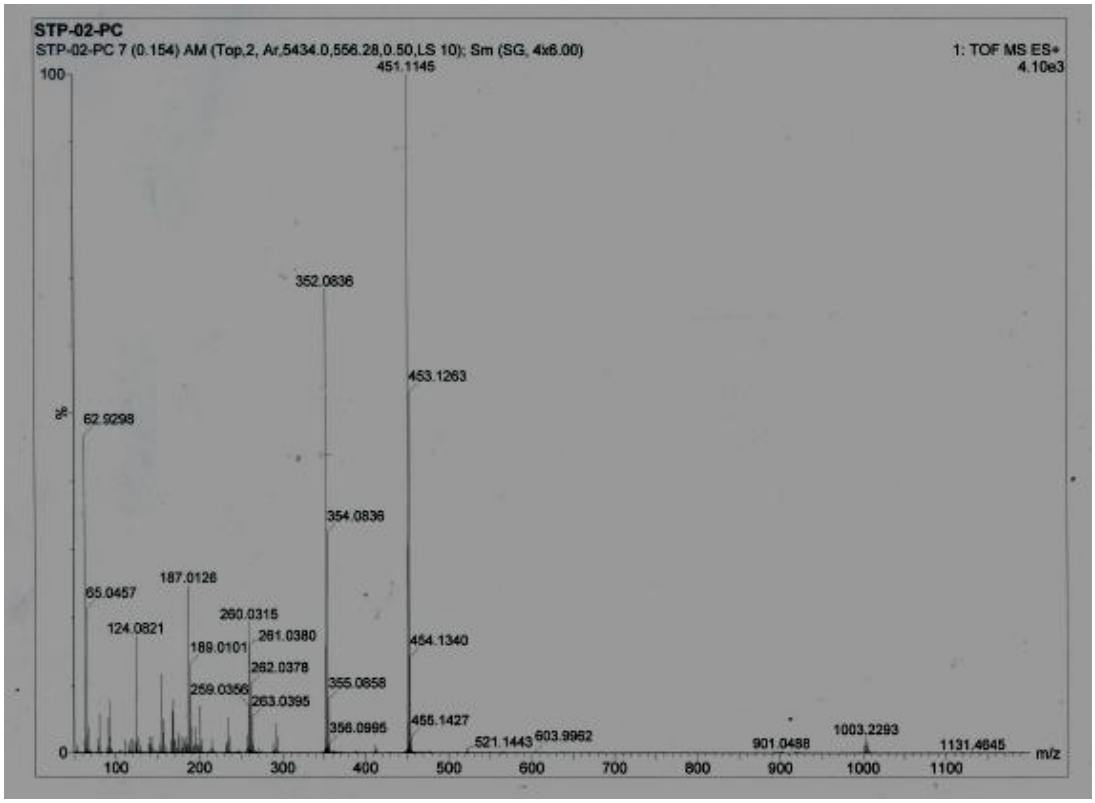

Fig. S1 ESI-MS spectrum of complex **1** in MeOH**.**

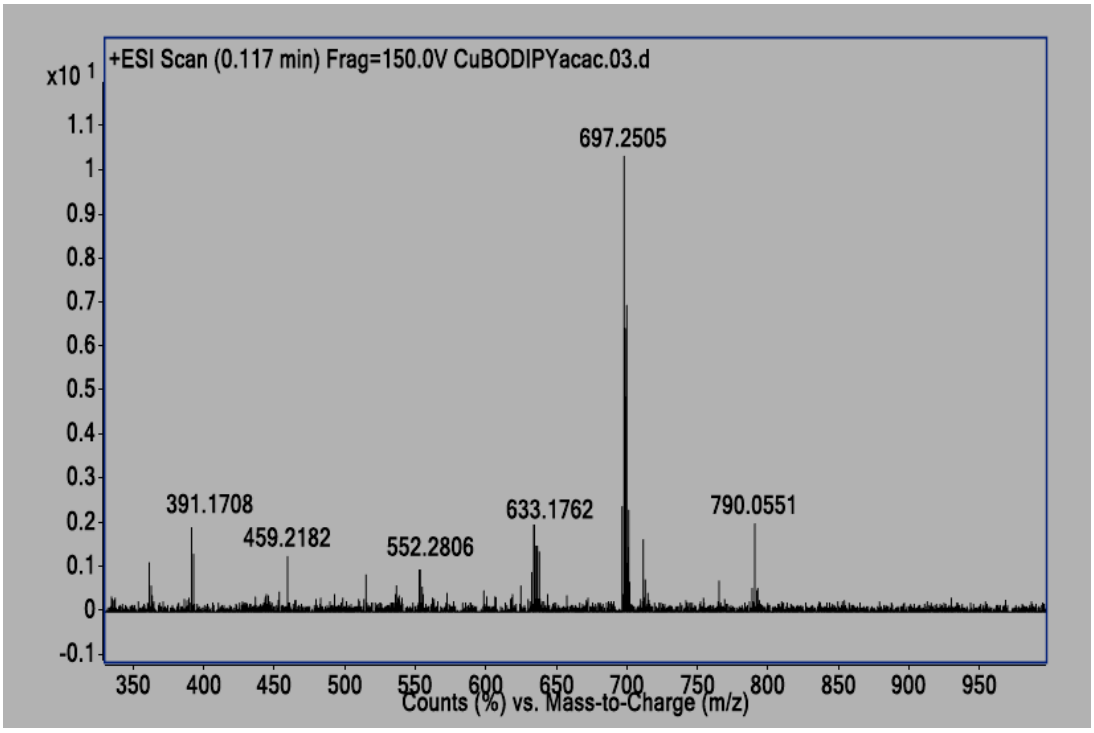

Fig. S2 ESI-MS spectrum of complex **2** in MeOH**.**

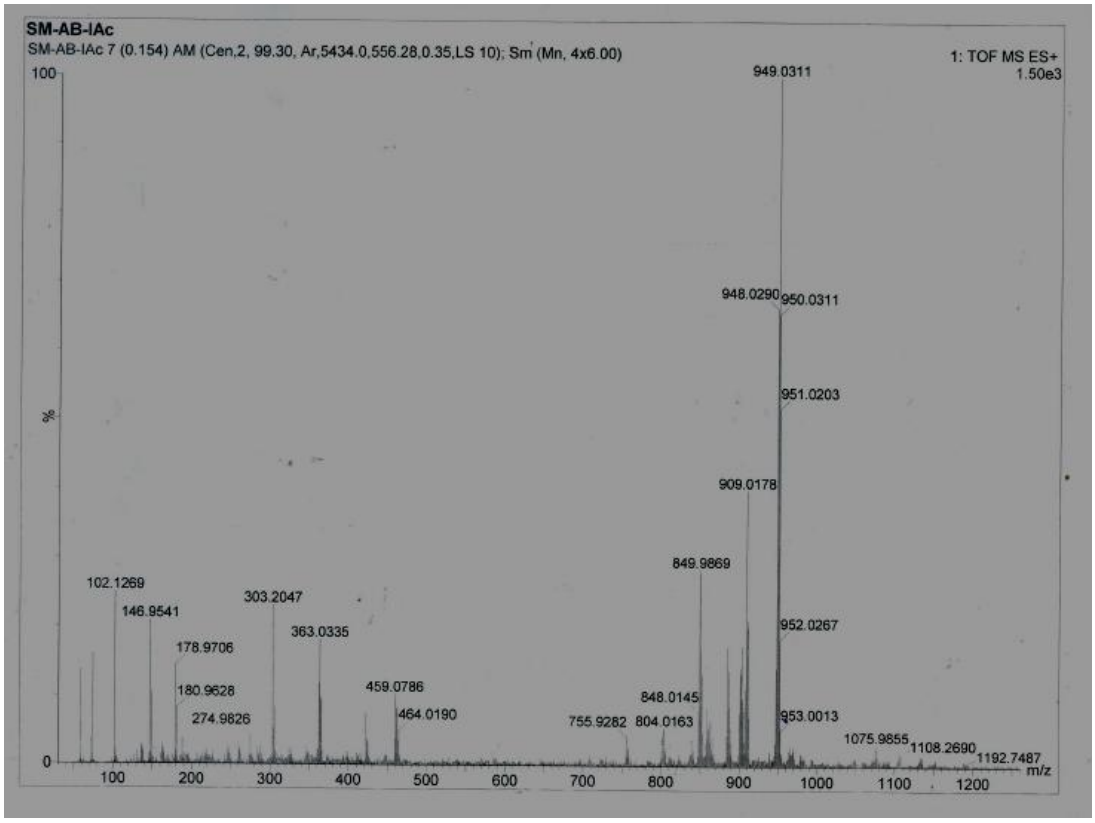

Fig. S3 ESI-MS spectrum of complex **3** in MeOH**.**

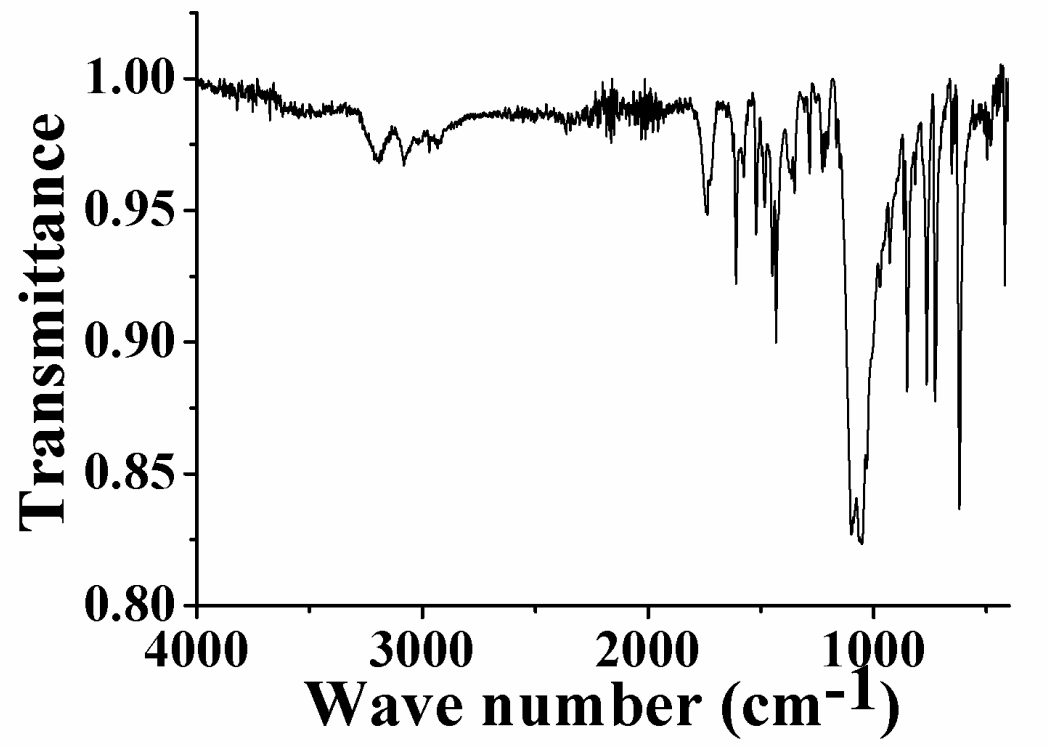

Fig. S4 IR spectrum of complex **1.**

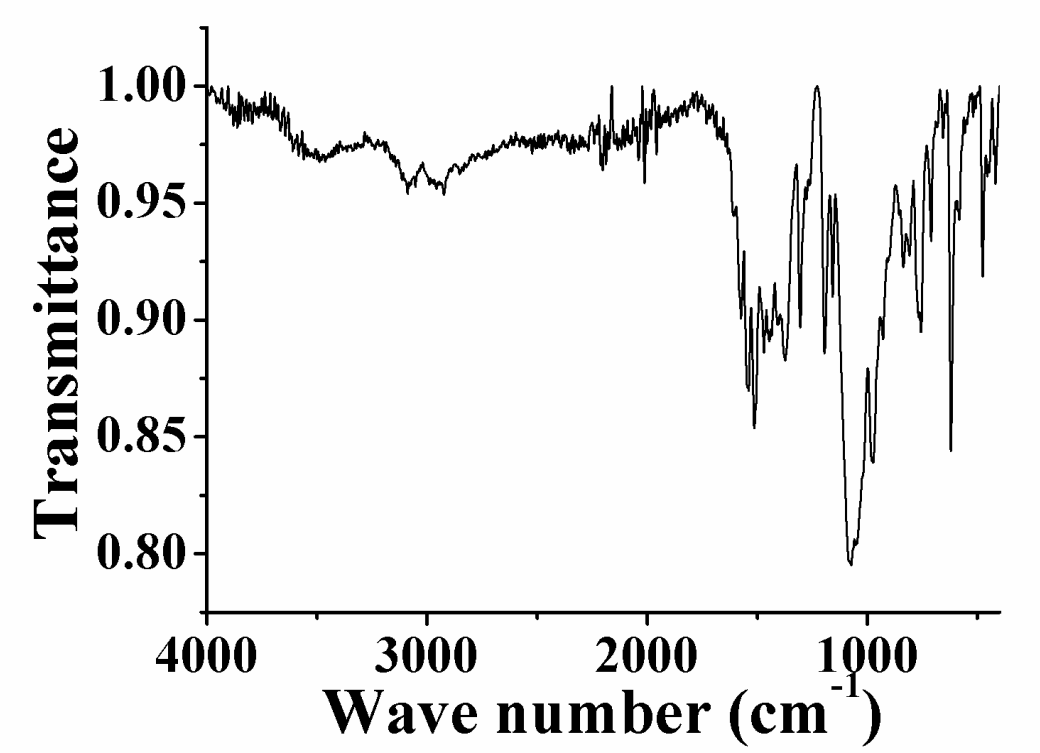

Fig. S5 IR spectrum of complex **2.**

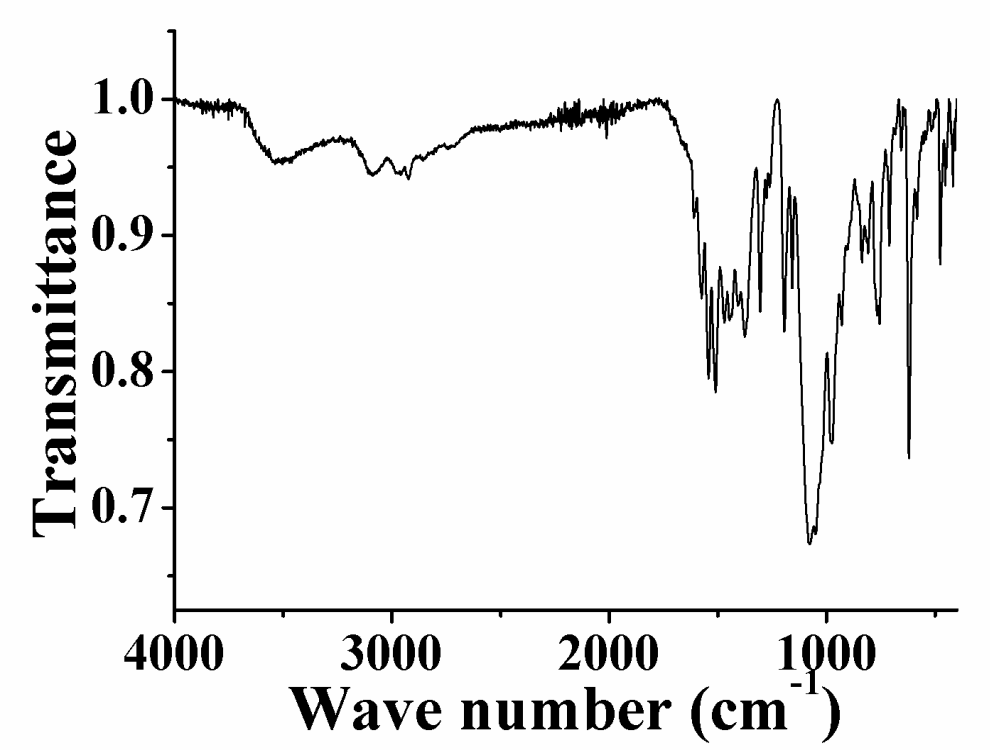

Fig. S6 IR spectrum of complex **3.**

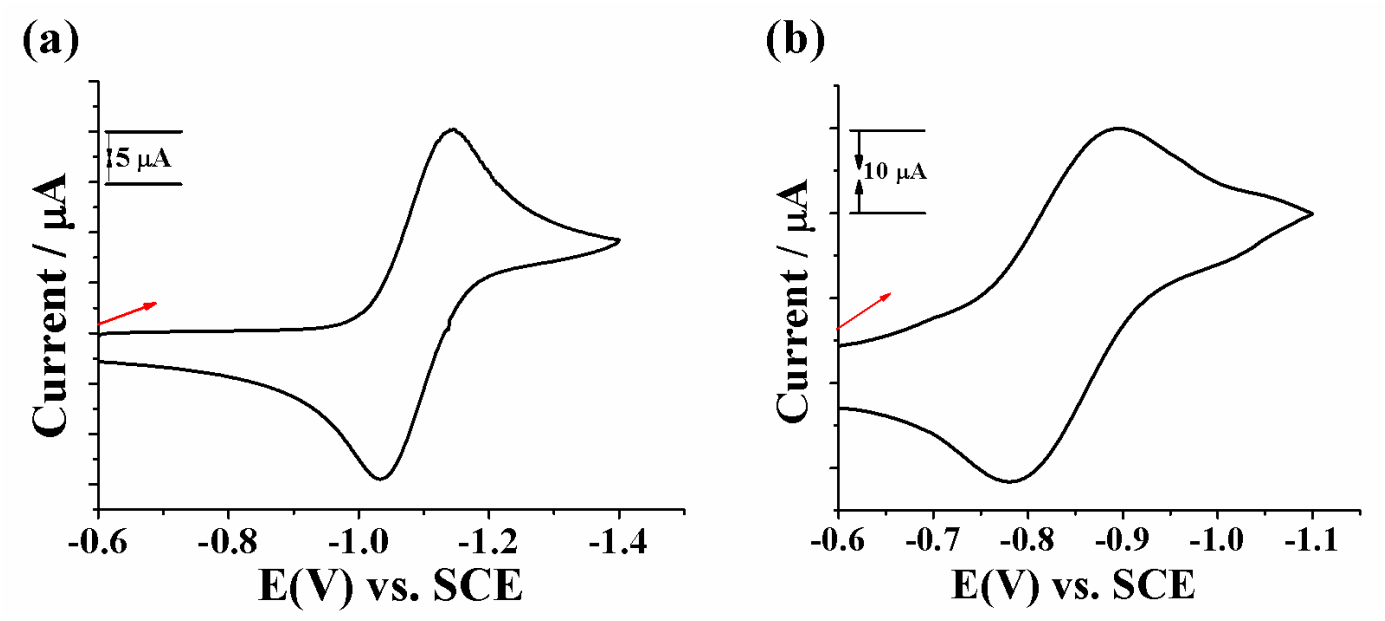

Fig. S7 Cyclic voltammogram of the BODIPY ligands $\mathbf{L^2}$ (a) and $\mathbf{L^3}$ (b) measured in DMF-0.1M TBAP. Sample concentration = 2.0 mmol, scan rate = 100 mV sec^{-1}, scan direction is cathodic.

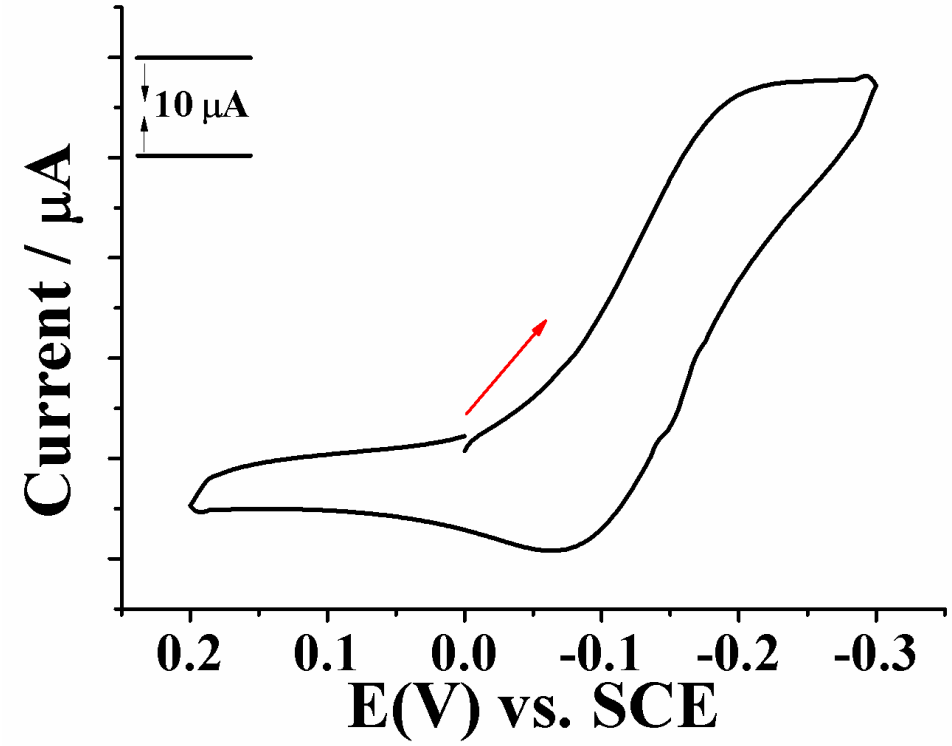

Fig. S8 Cyclic voltammogram of **1** for the Cu^{++}/Cu^{+} redox couple in 0.1M TBAP-DMF using 2.0 mmol complex concentration at a scan rate of 100 mV sec^{-1} and cathodic scan direction.

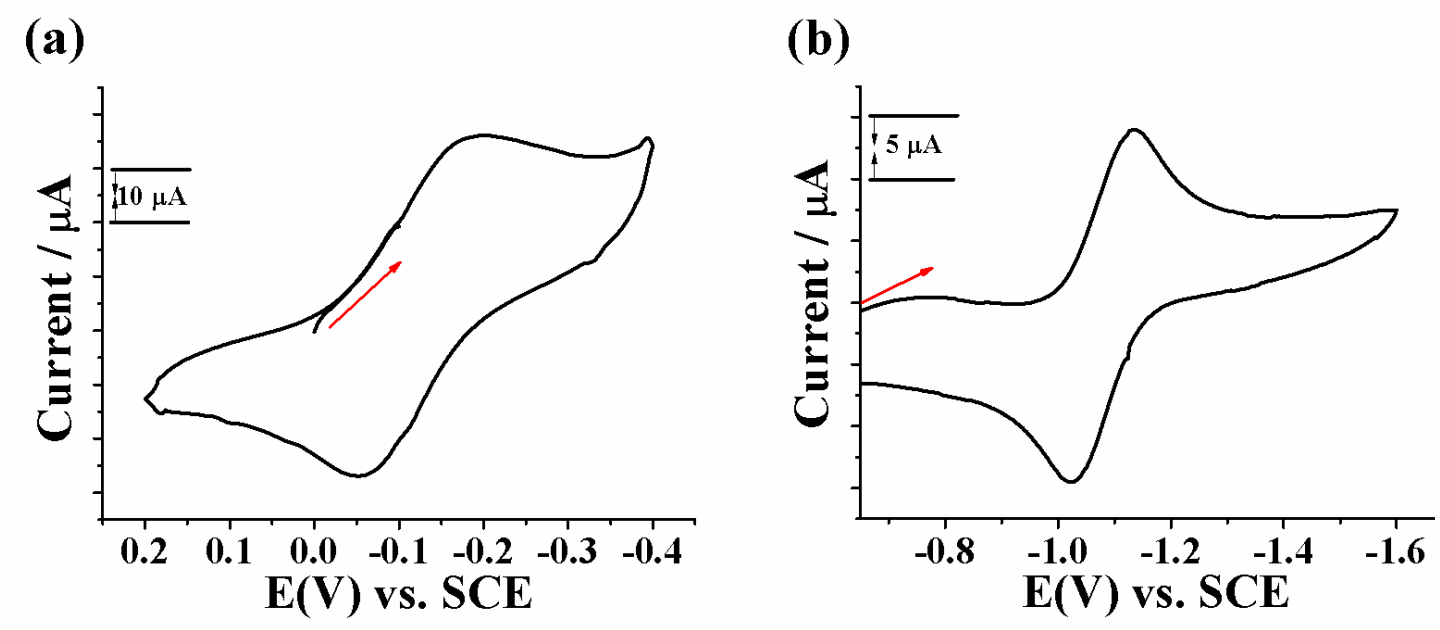

Fig. S9 Cyclic voltammogram of complex **2** (conc. = 2.0 mmol) in 0.1M TBAP-DMF showing (a) Cu^{2+}/Cu^{+} redox couple and (b) reduction of the BODIPY ligand L^2. Scan rate = 100 mV sec^{-1}. Scan direction is cathodic.

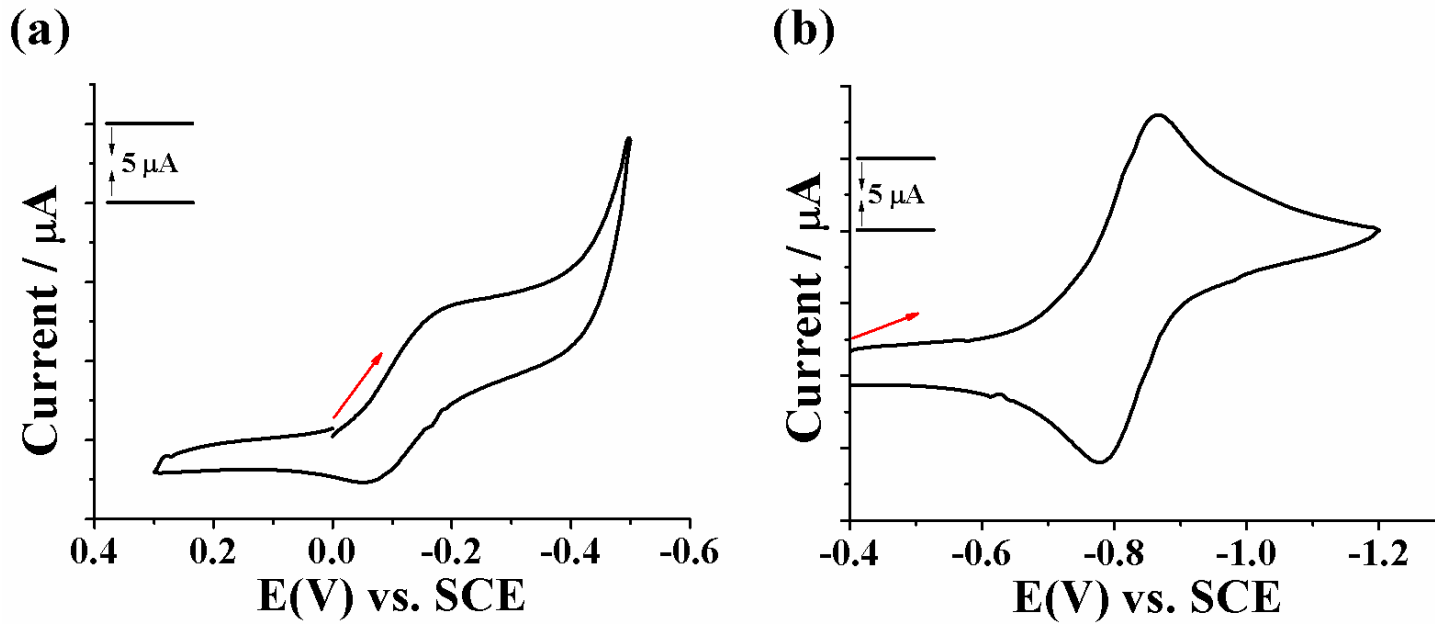

Fig. S10 Cyclic voltammogram of complex **3** (conc. = 2.0 mmol) in 0.1M TBAP-DMF showing (a) Cu^{2+}/Cu^{+} redox couple and (b) reduction of the BODIPY ligand L^3. Scan rate = 100 mV sec^{-1}. Scan direction is cathodic.

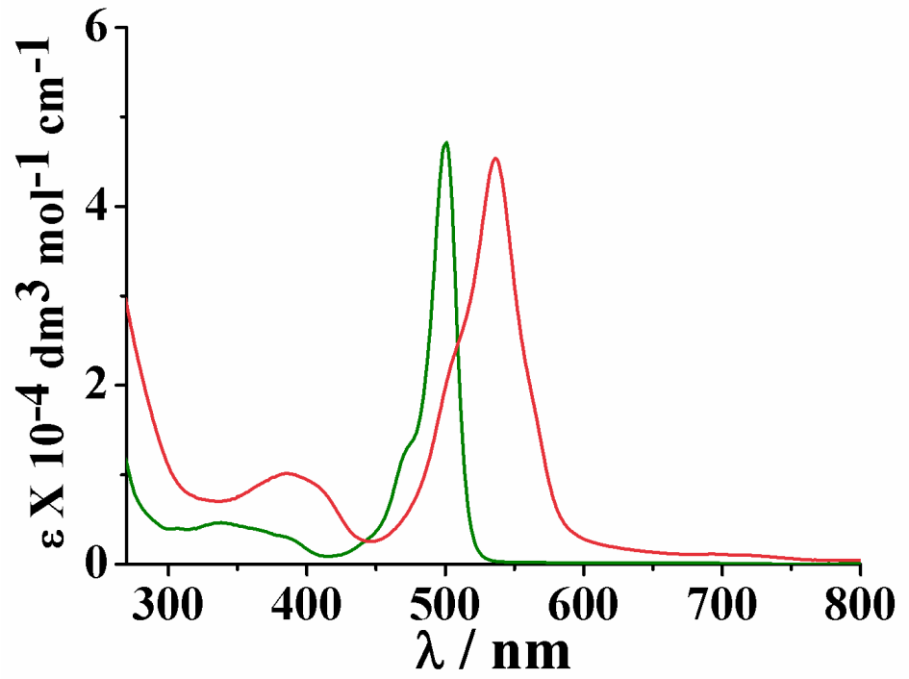

Fig. S11 UV-visible absorption spectra for the BODIPY ligands L^2 and L^3 in 5% DMSO-PBS buffer [Colour codes: L^2, green; L^3, red].

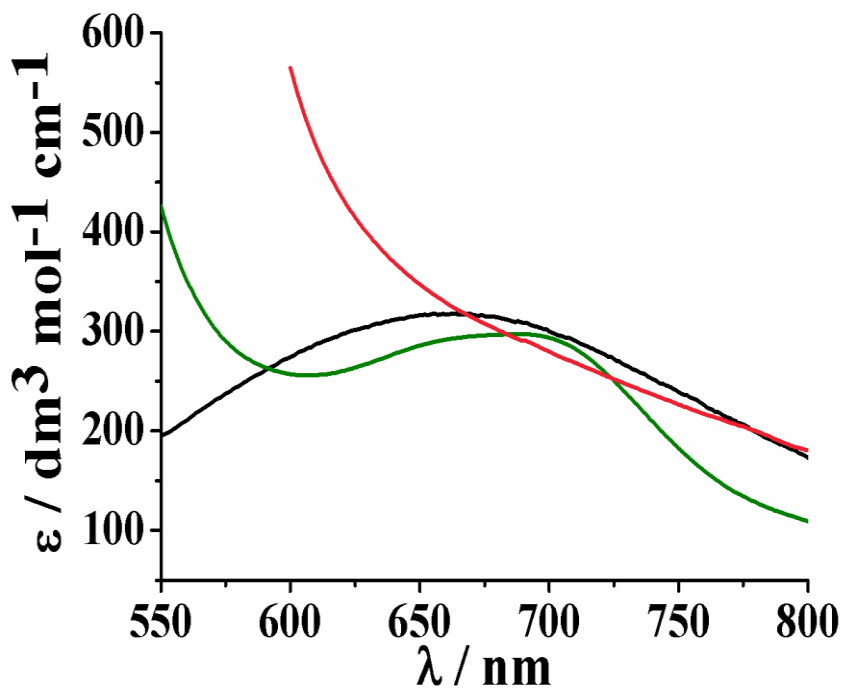

Fig. S12 UV-visible absorption spectra of complexes **1**-**3** in 5% DMSO-PBS buffer showing metal centred d-d transitions [Colour codes: complex **1**, black; complex **2**, green, complex **3**, red].

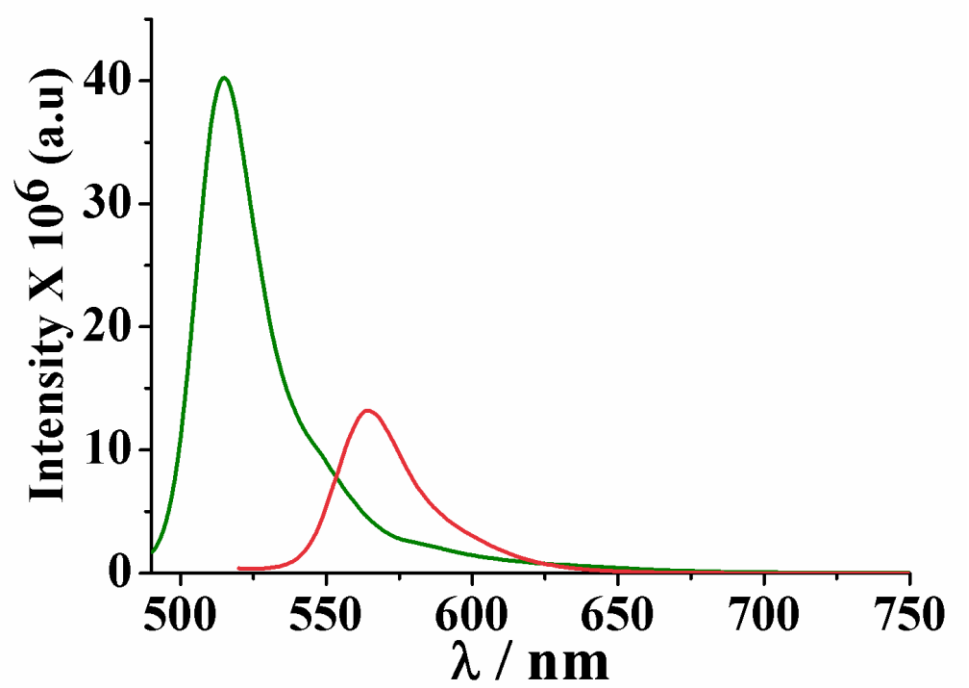

Fig.S13 Emission spectra for the BODIPY ligands L2 (green) and L3 (red) recorded in 5% DMSO-PBS buffer.

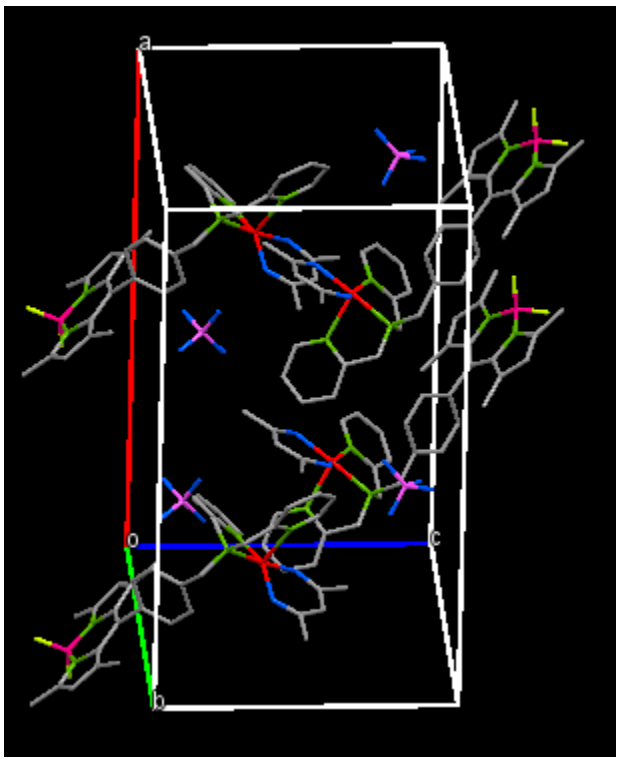

Fig. S14 Unit cell packing diagram of complex **2**. Colour codes: Copper, red; Nitrogen, green; Oxygen, blue; Carbon, grey; Chlorine, violet; boron, pink; fluorine, light green. Hydrogen atoms are omitted for clarity.

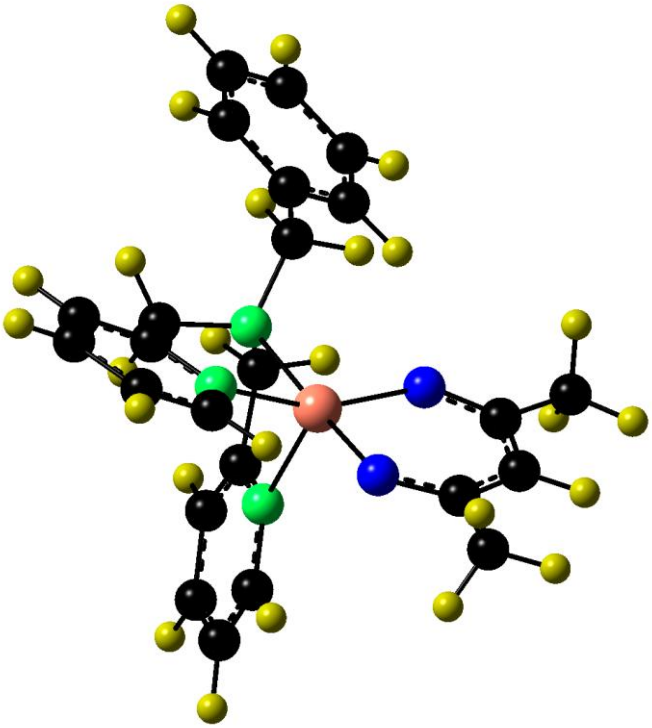

Fig. S15 Energy optimized structure of complex **1** [colour codes: copper, red; nitrogen, green; oxygen, blue; carbon, black and hydrogen, yellow].

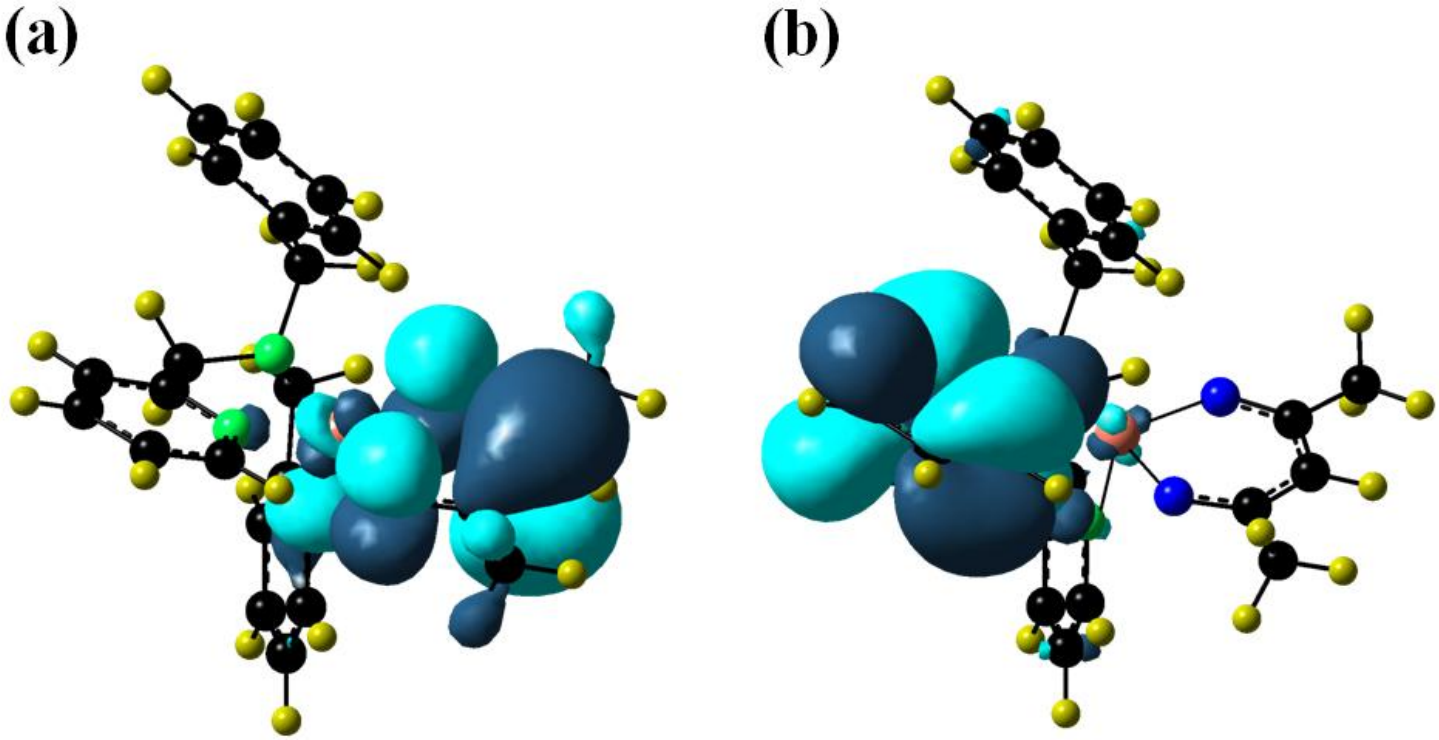

Fig. S16 HOMO (a) and LUMO (b) of complex **1** [Colour codes: Copper, red; nitrogen, green; oxygen, blue; carbon, black and hydrogen, yellow].

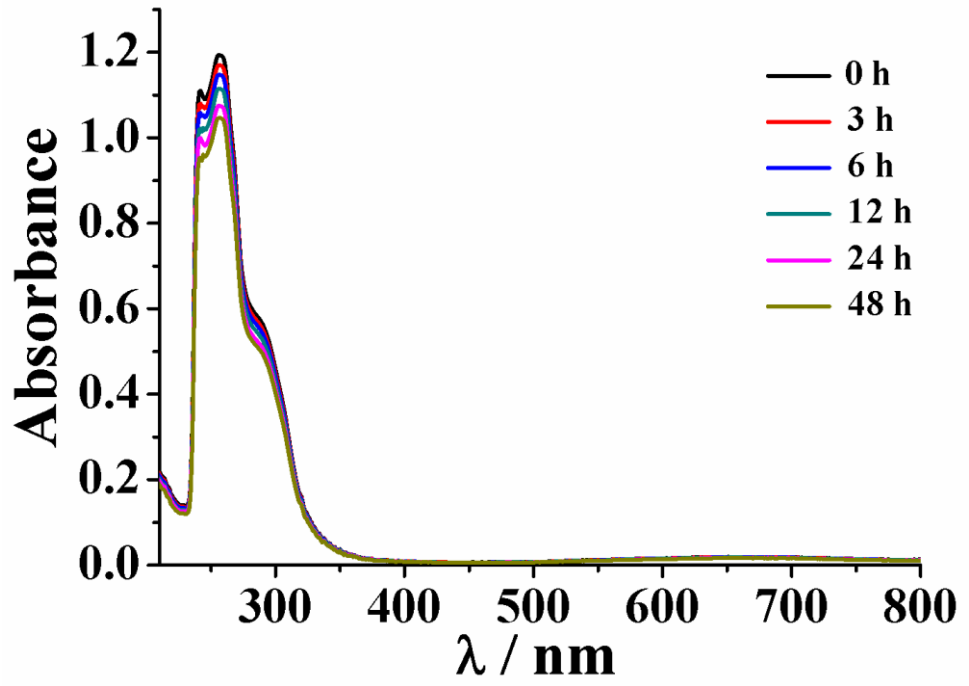

Fig. S17 Time dependent absorption spectra of complex **1** in 1:1 DMSO-PBS buffer (pH=7.2) measured up to 48 h for stability studies.

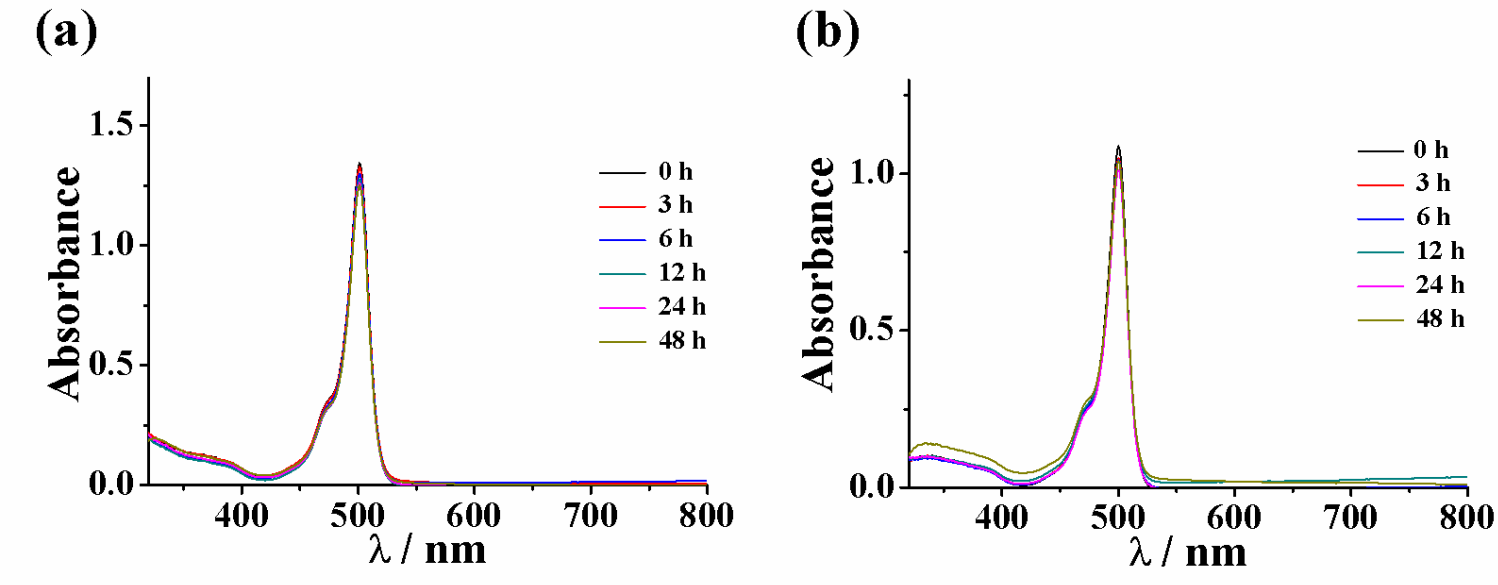

Fig. S18 Time dependent absorption spectra of complex **2** (a) and the corresponding BODIPY ligand L^2 (b) in 1:1 DMSO-PBS buffer (pH=7.2) measured up to 48 h for stability studies.

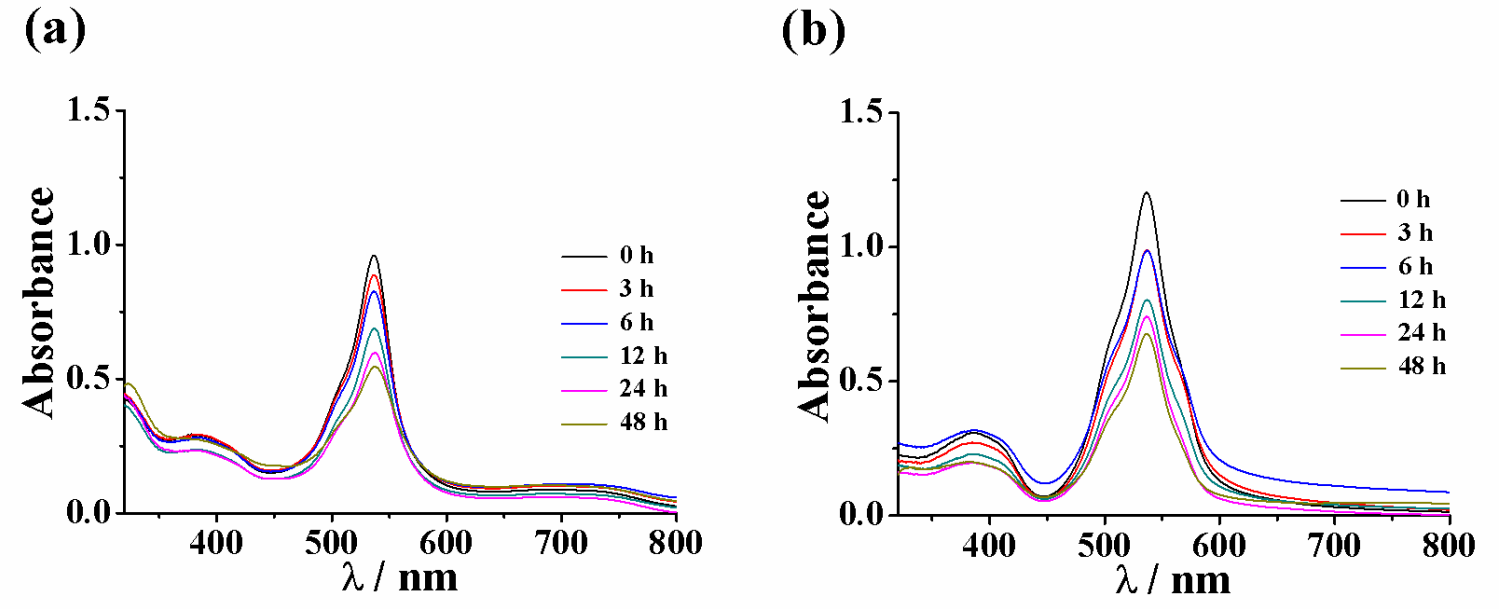

Fig. S19 Time dependent absorption spectra of complex **3** (a) and corresponding BODIPY ligand L^3 (b) in 1:1 DMSO-PBS buffer (pH=7.2) measured up to 48 h for stability studies.

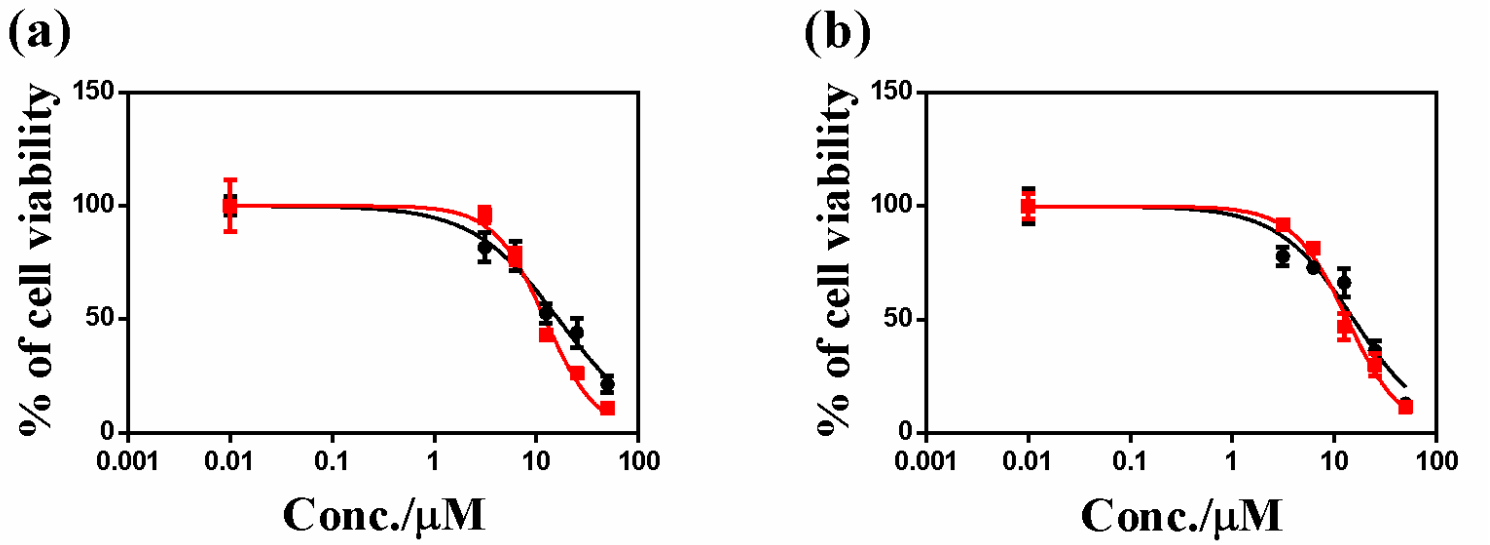

Fig. S20 MTT assay in HeLa cells (a) and in MCF-7 cells (b) treated with the complex **1** for 4 h, followed by 1 h incubation in the dark (black) or exposure to visible light (400–700 nm, red).

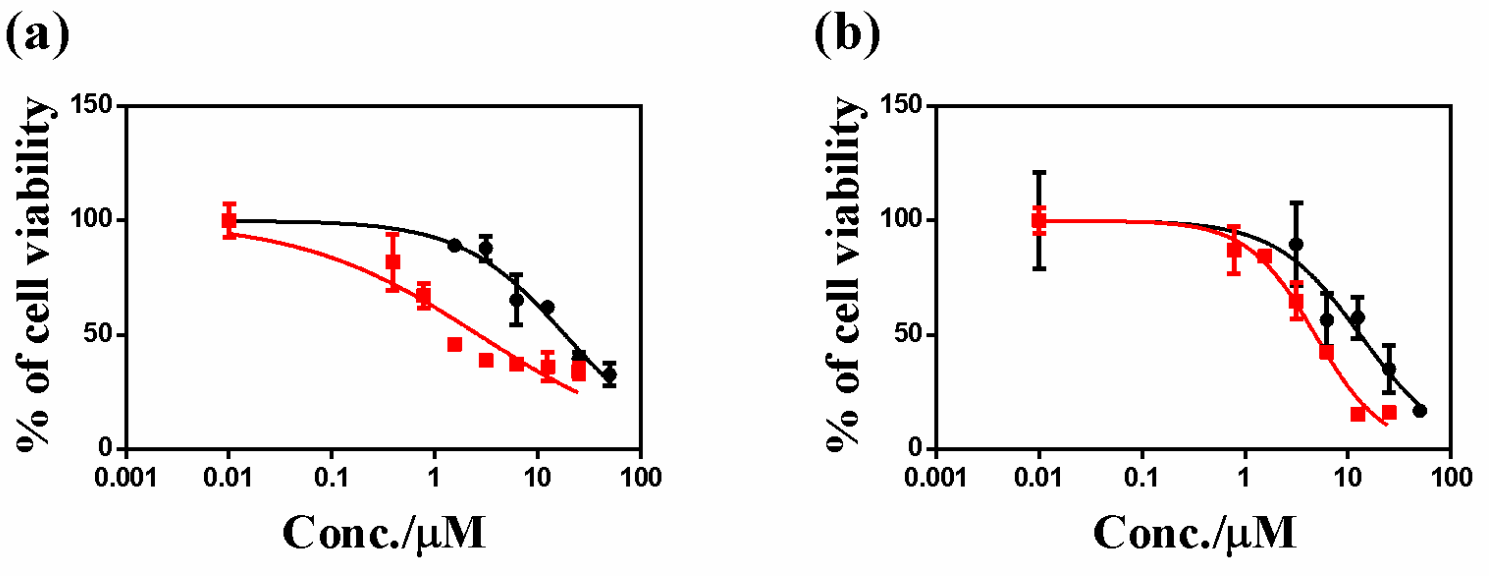

Fig. S21 MTT assay in HeLa cells (a) and in MCF-7 cells (b) treated with the complex **2** for 4 h, followed by 1 h incubation in the dark (black) or exposure to visible light (400–700 nm, red).

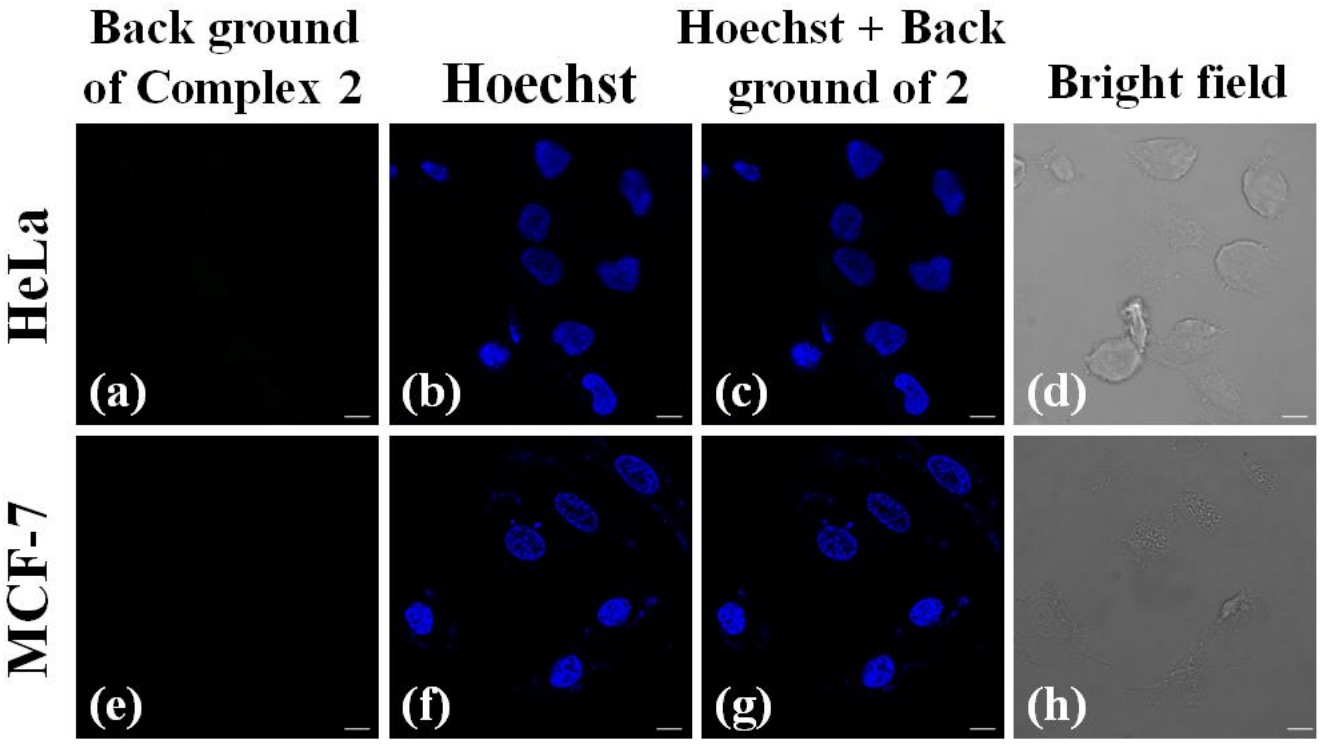

Fig. S22 Confocal microscopic images of HeLa and MCF-7 cancer cells taken after 4 h without the treatment of complex **2**. These images are taken as controls. Panels (b) and (f) indicate blue fluorescence of nuclear targeting Hoechst 33342 dye (5 μg mL^{-1}); panels (a) and (e) exhibit background green emission without **2**; panels (c) and (g) are the merged images of background green emission and Hoechst dye and panels (d) and (h) are the bright field images [scale bar = 10 μm].

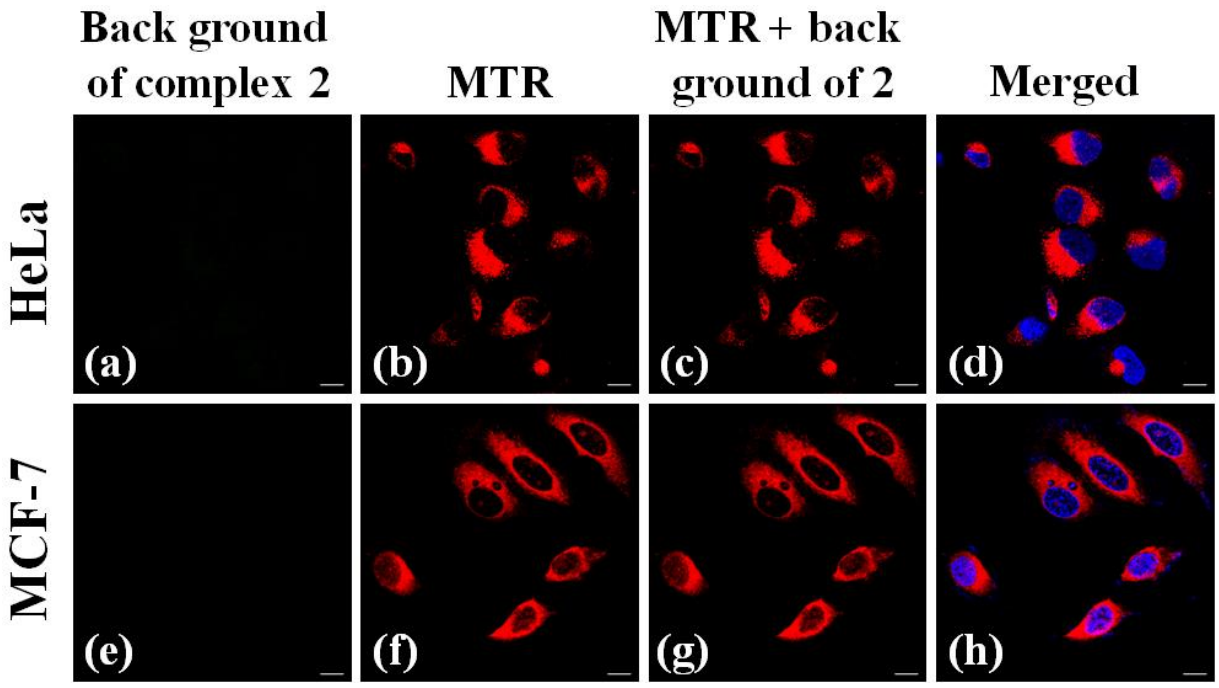

Fig. S23 Confocal microscopic images of HeLa and MCF-7 cells taken after 4 h with MitoTracker Red (MTR, 0.1 μM) and without the treatment of complex **2.** These images are taken as control. Panels (a) and (e) show the back ground green fluorescence without complex **2**, panels (b) and (f) display the red fluorescence of MTR; panels (c) and (g) are the merged images of MTR and the back ground emission of complex **2** and panels (d) and (h) are the merged pictures of Hoechst dye and MTR red with the back ground of complex **2**. Scale bar = 10 μm.

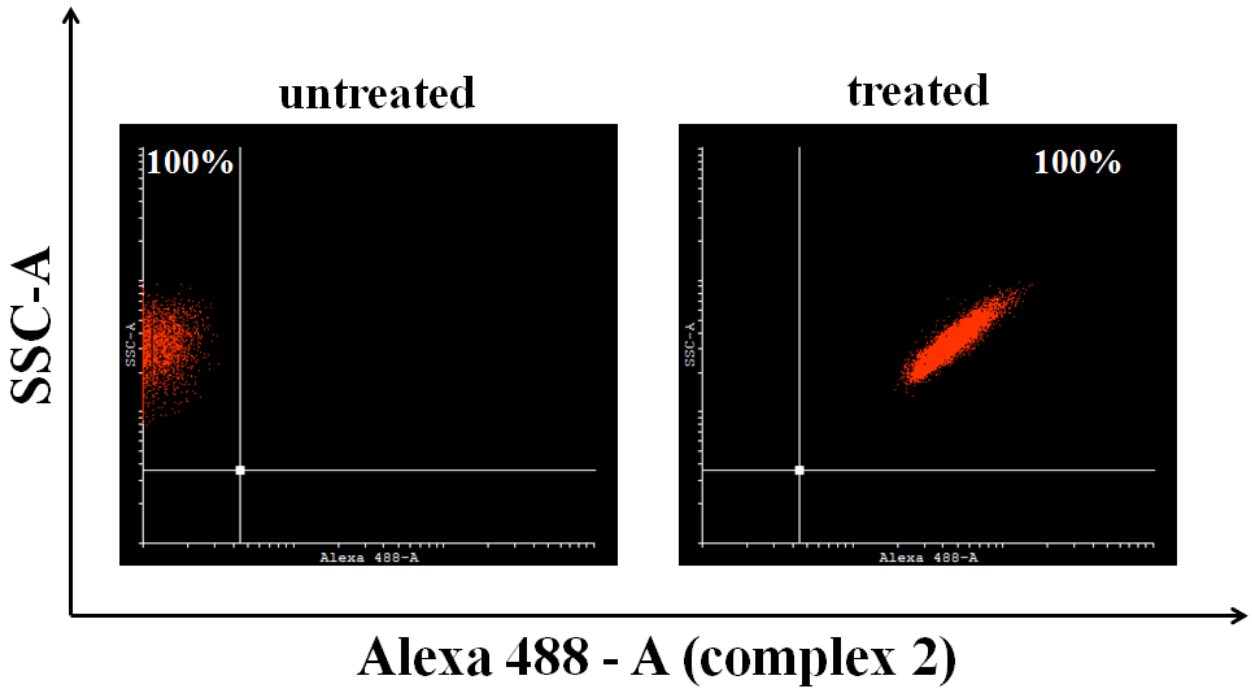

Fig. S24 Cellular uptake data for complex **2** in HeLa cells using FACS analysis. Dot plot on the left shows untreated cells while plot on the right shows HeLa cells treated with complex **2** (1.0 μM) for 4 h. The data show ~100% accumulation of the complex inside HeLa cells after 4 h.

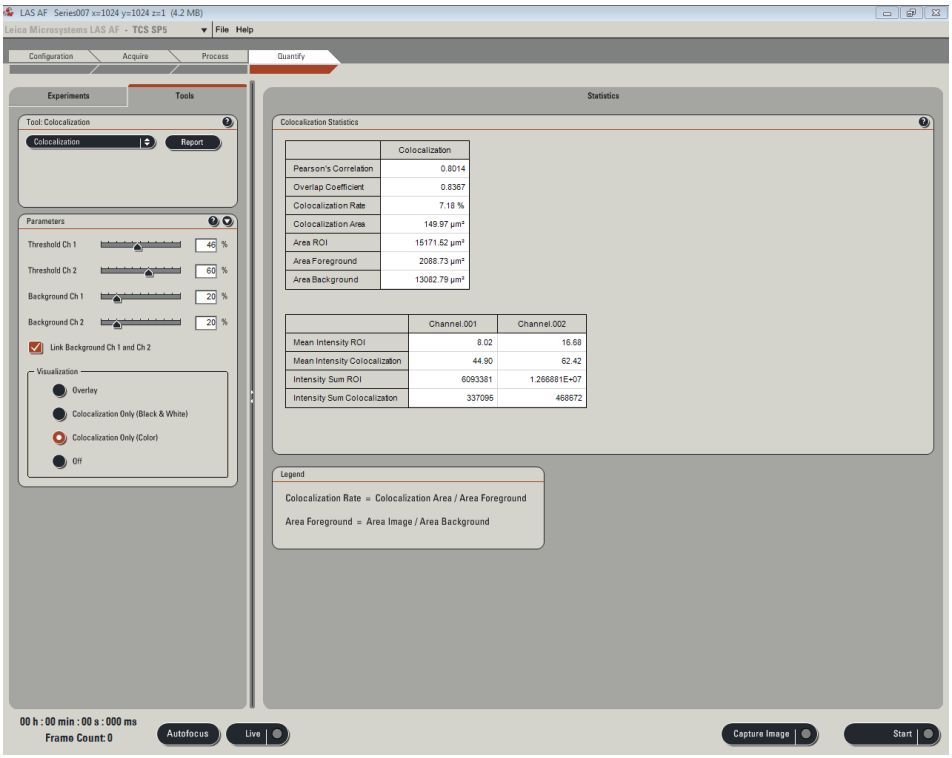

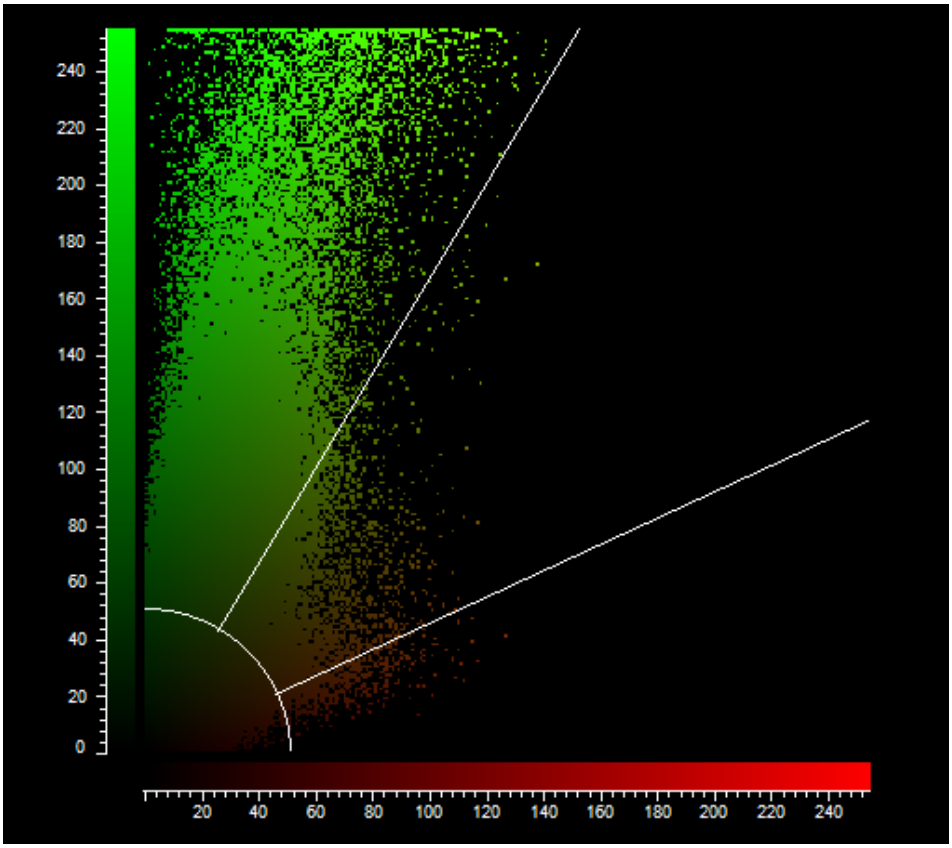

Fig. S25 Calculations and plots for the determination of Pearson's and overlap coefficients of complex **2** inside the mitochondria of the HeLa cells.

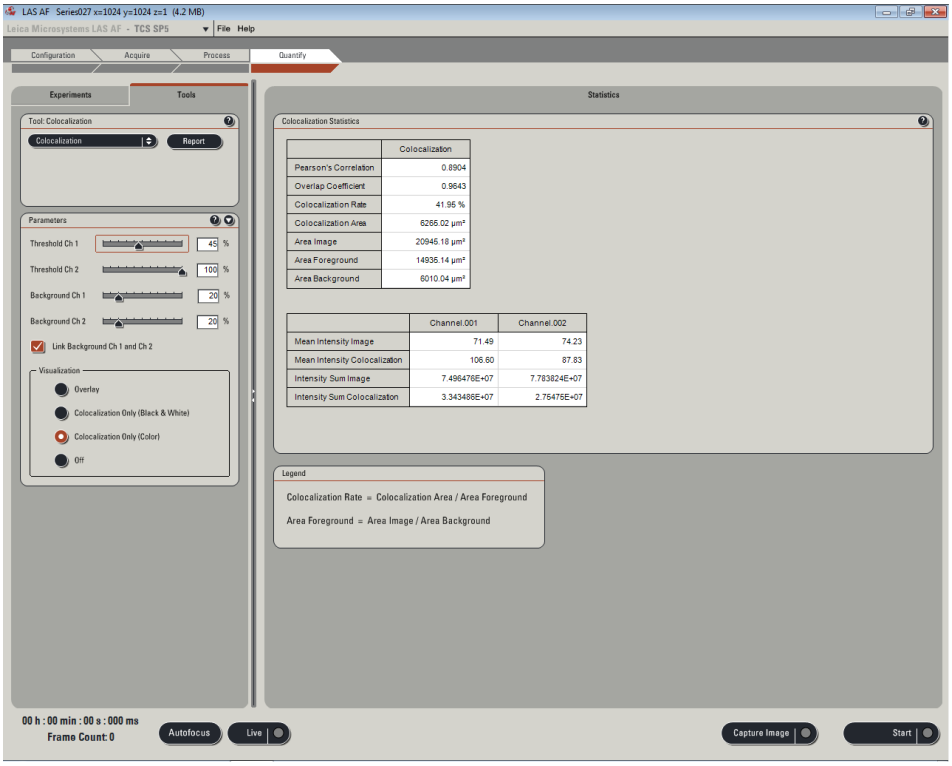

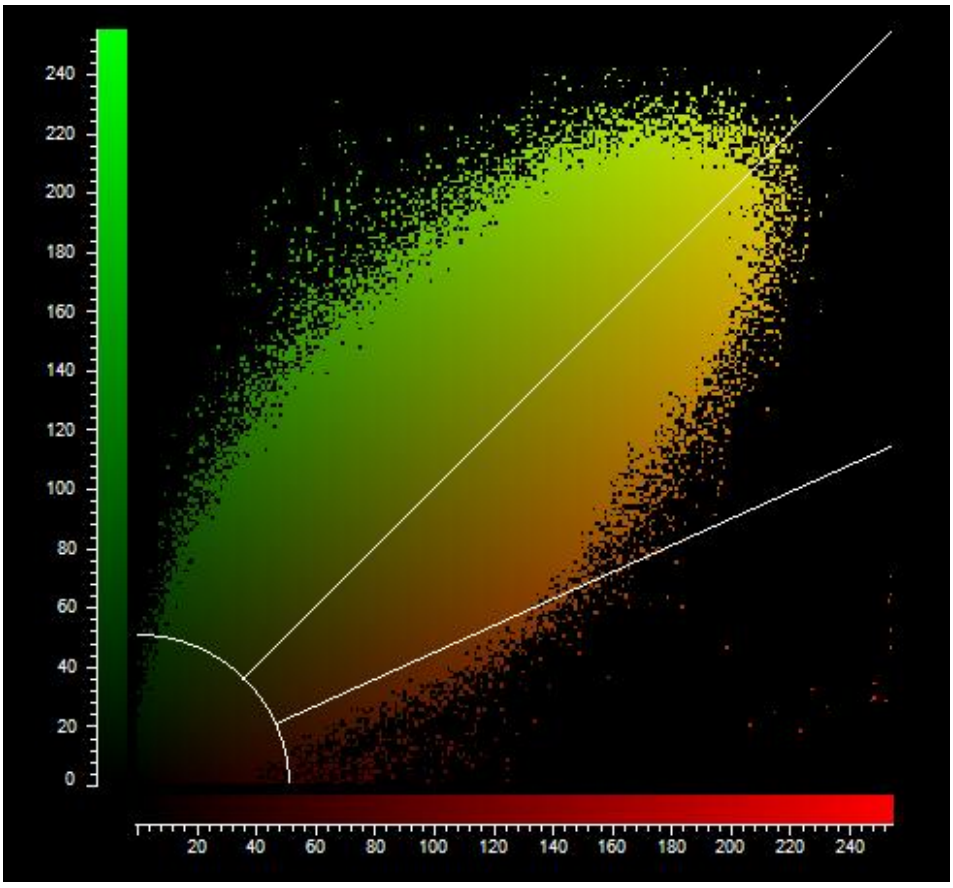

Fig. S26 Calculations and plots for the determination of Pearson's and overlap coefficients of complex **2** inside the mitochondria of the MCF-7 cells.

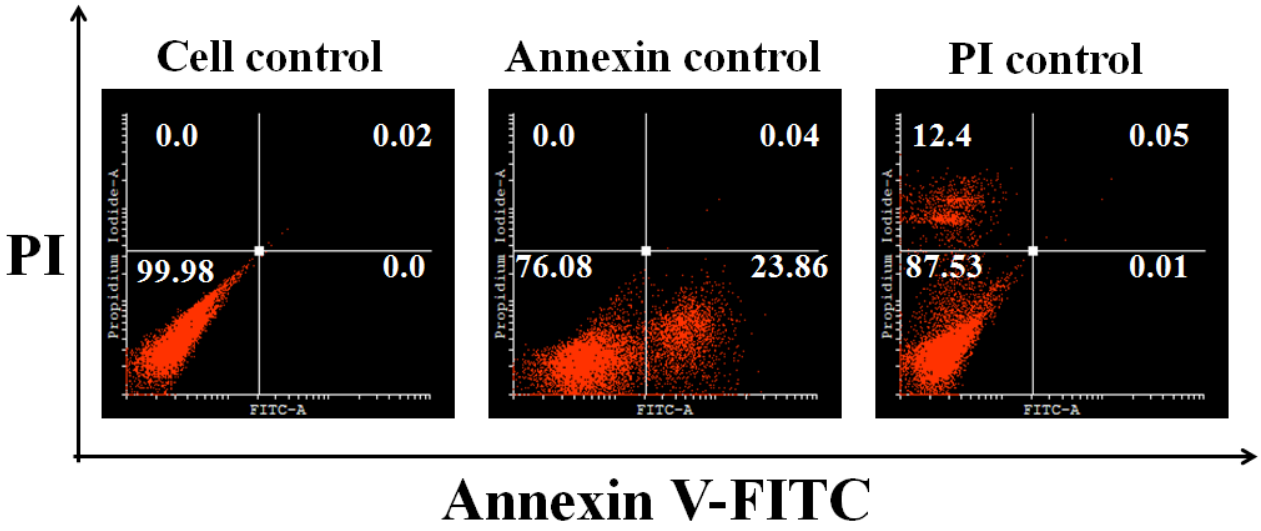

Fig. S27 FACS analysis data for different controls used in Annexin V-FITC/PI assay for complex **3.**

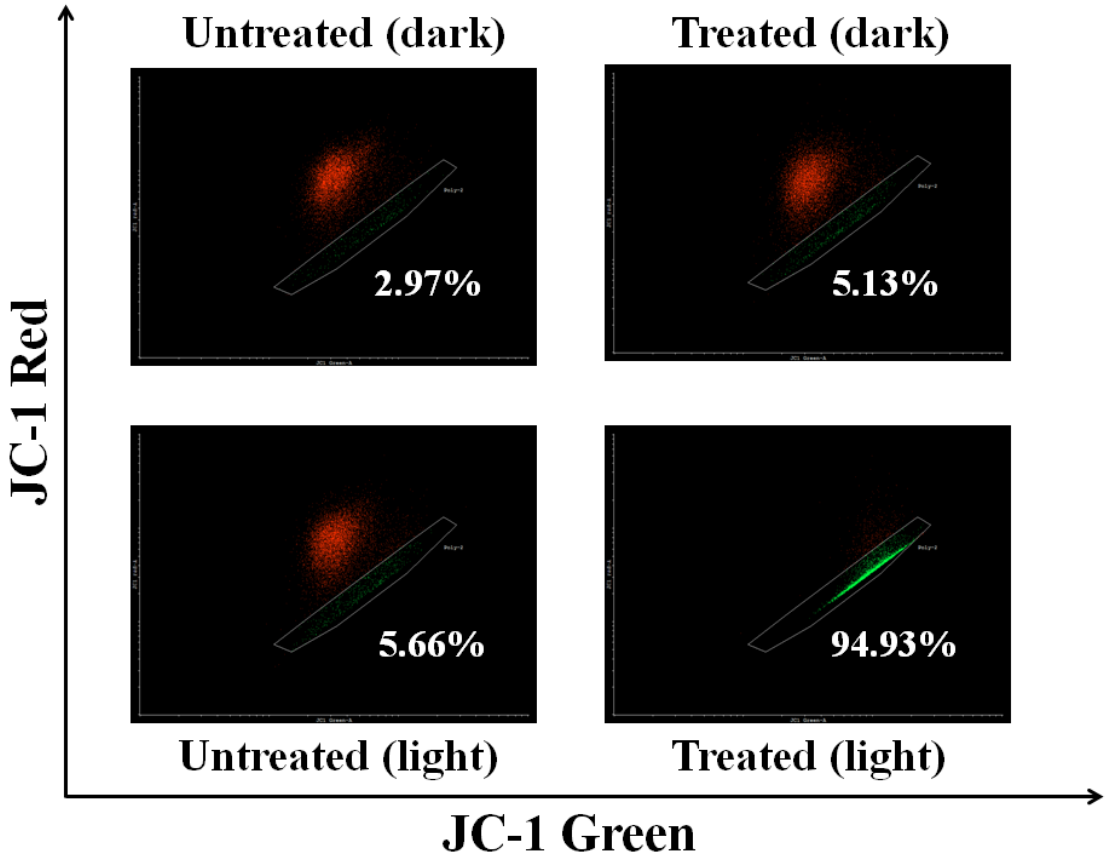

Fig. S28 Plot for JC-1 assay for complex **3** in HeLa cells using FACS analysis. Upper left panel shows HeLa cells with JC-1 dye alone kept in dark condition. Lower left panel shows HeLa cells with JC-1 dye alone after visible light irradiation (400-700 nm, 1 h).Upper right panel shows HeLa cells with JC-1 dye after treatment of complex **3** (0.05 μM) in dark for 4 h while lower right panel shows HeLa cells with JC-1 dye after treatment of complex **3** (0.05 μM) for 4 h followed by irradiation for 1 h in visible light (400-700 nm). Digits indicate the percentage of cells giving green fluorescence of JC-1 dye originating due to the change of mitochondrial membrane potential.

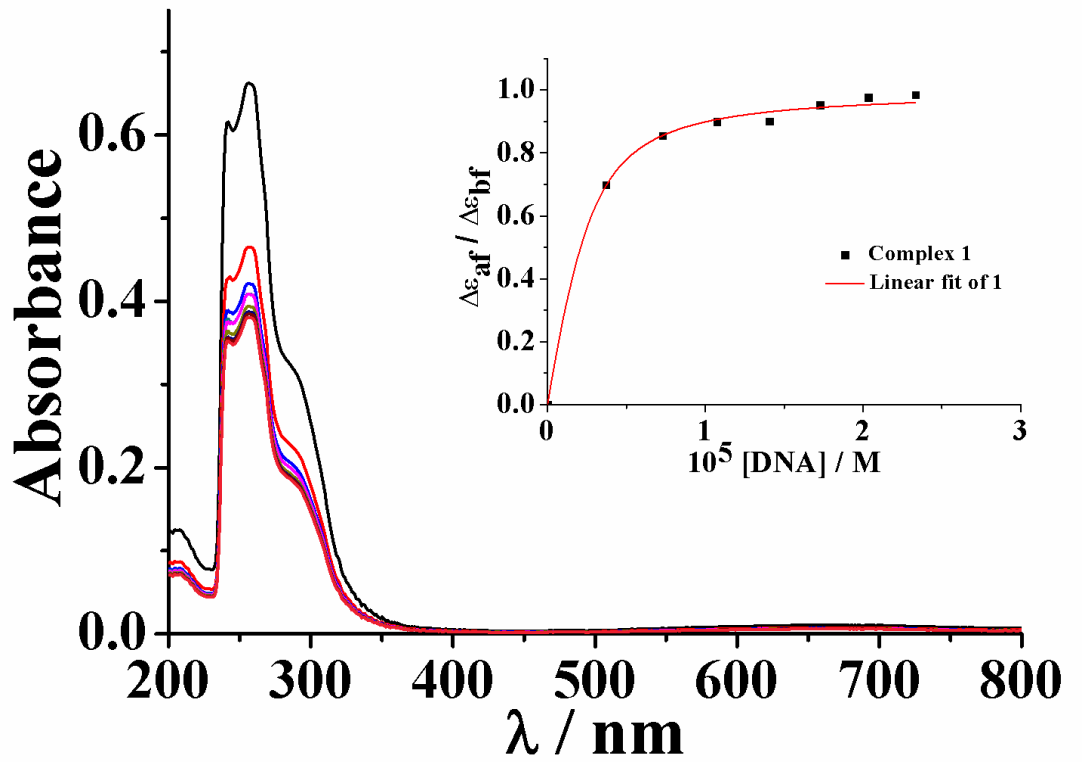

Fig. S29 Absorption spectral traces of complex **1** in 5 mM Tris-HCl buffer (pH 7.2) on increasing the quantity of calf thymus DNA. The inset shows the least-squares fit of $\Delta\varepsilon_{af}/\Delta\varepsilon_{bf}$ vs. [DNA] for complex **1** using McGhee-von Hippel (MvH) method.

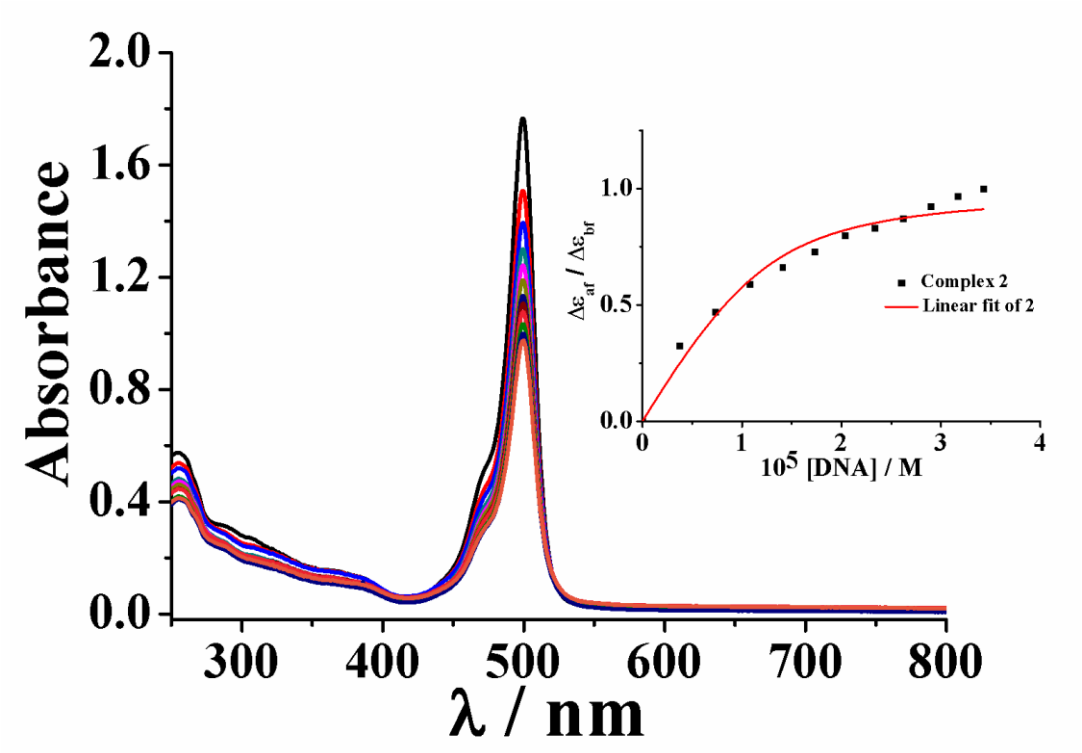

Fig. S30 Absorption spectral traces of complex **2** in 5 mM Tris-HCl buffer (pH 7.2) on increasing the quantity of calf thymus DNA. The inset shows the least-squares fit of $\Delta\varepsilon_{af}/\Delta\varepsilon_{bf}$ vs. [DNA] for complex **2** using McGhee-von Hippel (MvH) method.

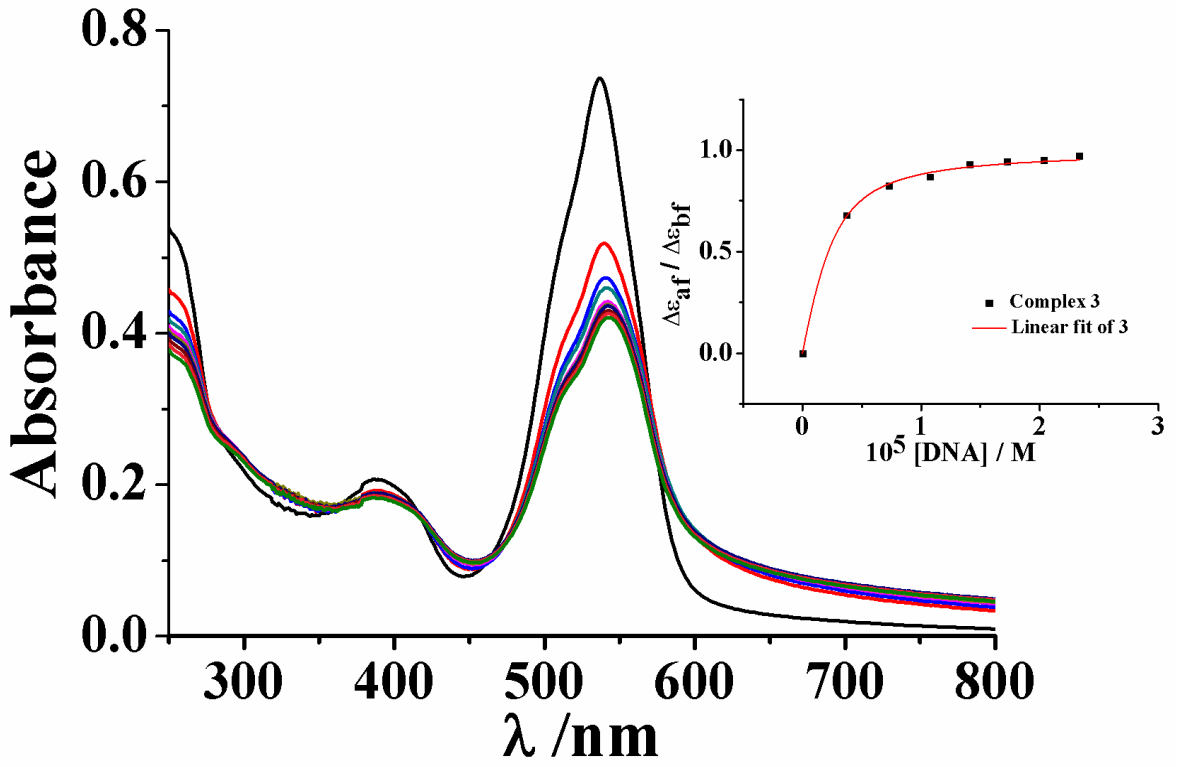

Fig. S31 Absorption spectral traces of complex **3** in 5 mM Tris-HCl buffer (pH 7.2) on increasing the quantity of calf thymus DNA. The inset shows the least square fit of $\Delta\varepsilon_{af}$ /$\Delta\varepsilon_{bf}$ vs. [DNA] for complex **3** using McGhee-von Hippel (MvH) method.

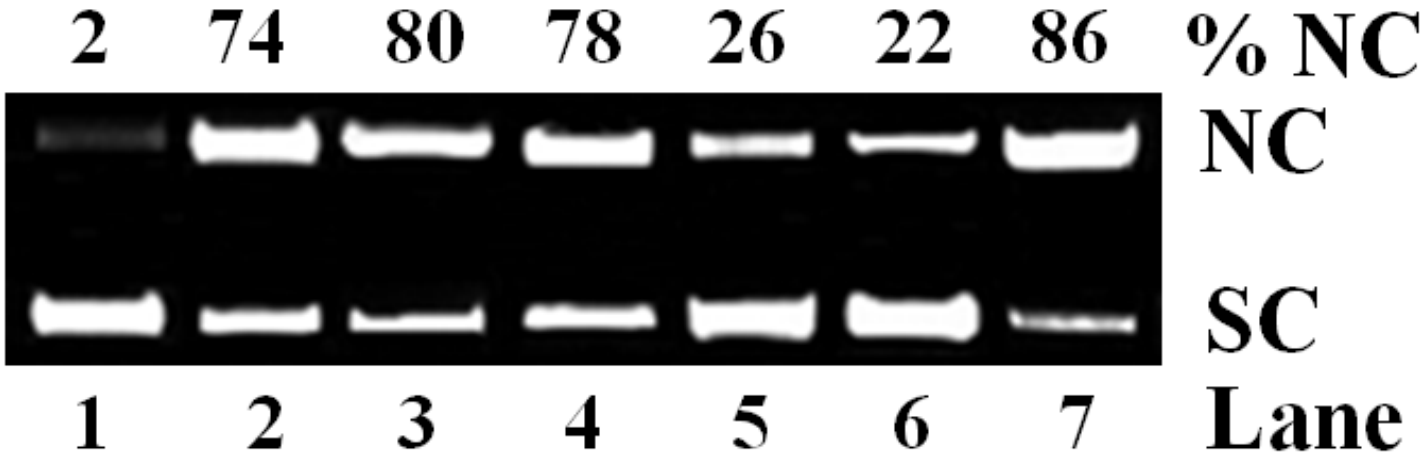

Fig. S32 Gel diagram showing photocleavage of pUC19 DNA (0.2 μg, 30 μM base pair) by complex **3** (5 μM) in visible light of 532 nm (1 h exposure) in the presence of different additives: KI, 4 mM; DMSO, 4 μl; catalase, 4 units; NaN_3, 4 mM; TEMP, 4 mM and SOD, 4 units (total volume = 20 μL). The lanes are: (1) DNA, (2) DNA + complex + KI, (3) DNA + complex + DMSO, (4) DNA + complex + catalase, (5) DNA + complex + NaN_3, (6) DNA + complex + TEMP, (7) DNA + complex + SOD.

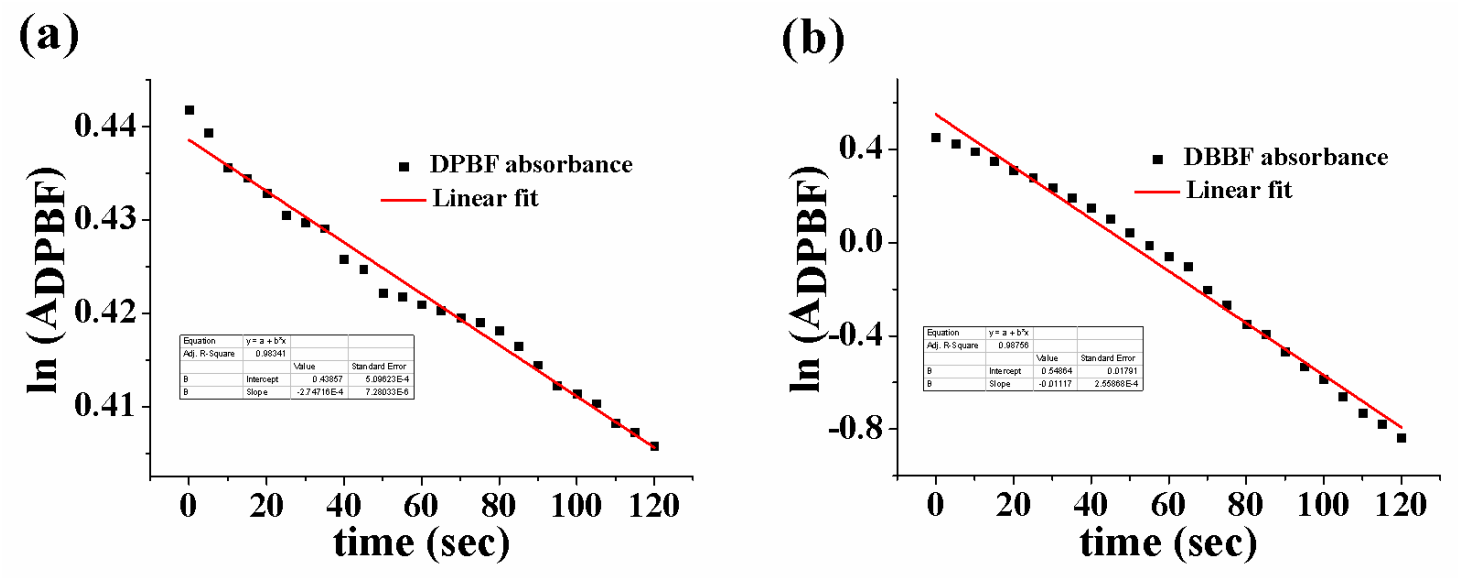

Fig. S33 Plot for determination of rate constant for the 1st order decay of DPBF in presence of complex **2** (a) and complex **3** (b) after irradiation with visible light of 400-700 nm.

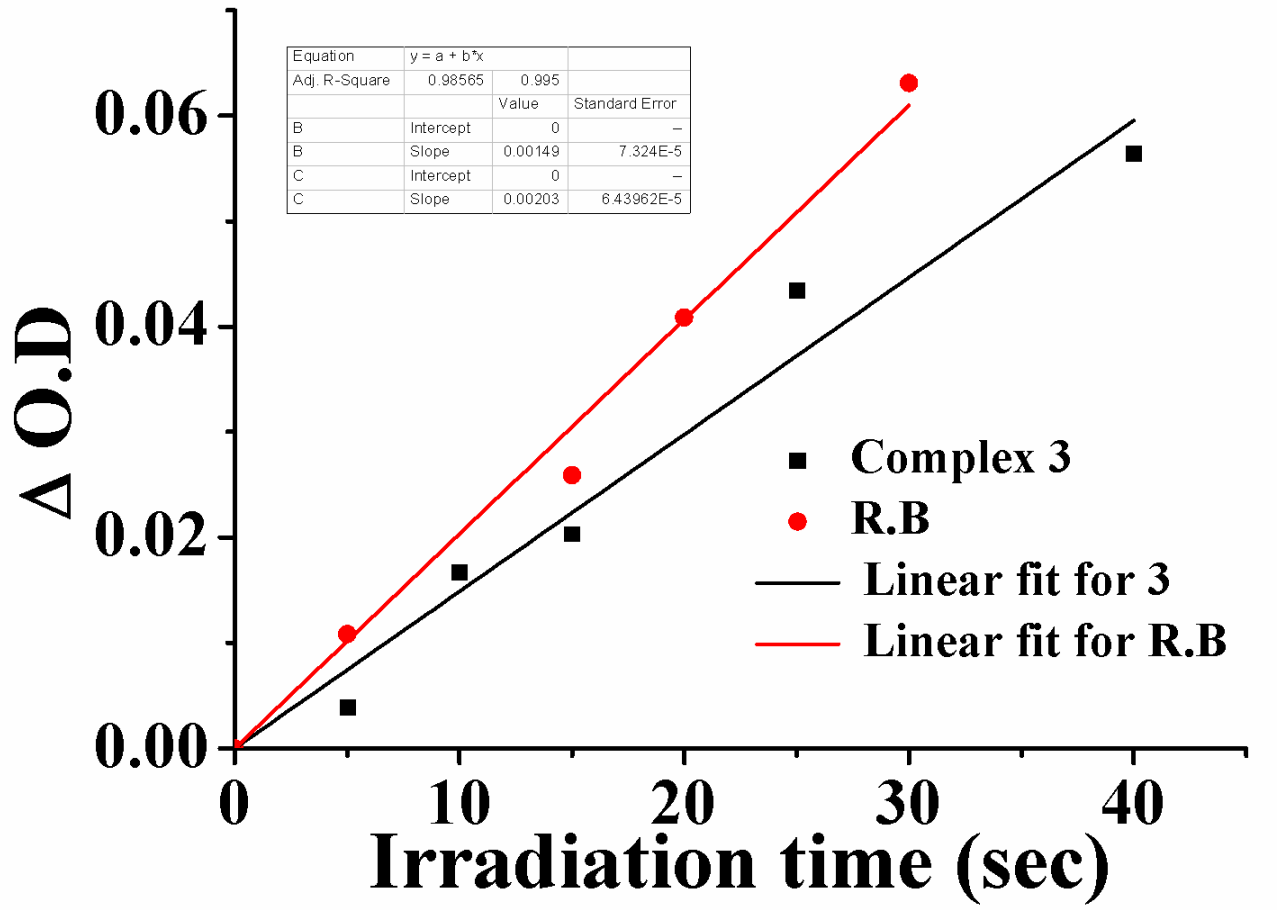

Fig. S34 Plot of change in absorbance of DPBF at ~416 nm vs. irradiation time in presence of Rose Bengal (RB) (red) and complex **3** (black) respectively for the determination of the singlet oxygen generation quantum yield of complex **3**.

Table S1. Selected bond distances (Å) and bond angles (°) of the crystal of complex **2**

Entry	**Complex 2**
O1 Cu1	1.912(3)
Cl1 O6	1.345(9)
Cu1 N3	1.980(4)
Cu1 N1	2.059(5)
Cu1 N2	2.225(4)
F1 B1	1.406(7)
F2 B1	1.382(7)
N5 B1	1.533(10)
N4 B1	1.524(11)
N1 C6	1.483(7)
N3 C1	1.344(7)
C34 O1 Cu1	123.5(3)
C36 O2 Cu1	122.8(4)
O3 Cl1 O6	99.7(13)
O3 Cl1 O5	111.3(10)
O1 Cu1 O2	94.51(17)
O1 Cu1 N3	92.61(15)
O2 Cu1 N3	157.99(15)
O1 Cu1 N1	174.54(17)
O2 Cu1 N1	90.15(19)
N3 Cu1 N1	84.06(17)
O1 Cu1 N2	97.61(15)
O2 Cu1 N2	92.85(16)
N3 Cu1 N2	106.81(16)
N1 Cu1 N2	79.29(17)
C12 N1 Cu1	106.9(3)
C25 N4 B1	127.8(6)
F2 B1 F1	108.6(5)
F2 B1 N4	110.2(6)
F1 B1 N4	108.4(6)
F2 B1 N5	111.4(6)
F1 B1 N5	111.0(6)
N4 B1 N5	107.2(5)
N1 C12 C11	112.6(4)

Table S2. List of coordinates for energy minimized structure of complex **1**

Center Number	Atomic Number	Atomic Type	Coordinates (Angstroms) X	Y	Z
1	8	0	0.970496	1.607639	1.597679
2	8	0	1.139305	1.527492	-1.227631
3	6	0	1.582513	2.759067	1.436803
4	6	0	1.976997	3.292101	0.188386
5	1	0	2.481532	4.250175	0.191958
6	6	0	1.847774	3.532003	2.711926
7	1	0	2.395058	2.899871	3.421971
8	1	0	0.893939	3.799745	3.185158
9	1	0	2.419104	4.445361	2.528944
10	6	0	1.741563	2.683514	-1.065169
11	6	0	2.184662	3.369136	-2.340629
12	1	0	1.318958	3.529066	-2.995800
13	1	0	2.886212	2.721996	-2.882508
14	1	0	2.666145	4.330625	-2.146352
15	29	0	0.495905	0.321327	0.191349
16	7	0	-0.227172	-1.019404	-1.285267
17	6	0	-1.379776	-1.757377	0.821915
18	7	0	-0.785784	-0.675089	1.389622
19	6	0	-1.113586	-0.283941	2.647256
20	1	0	-0.589450	0.589325	3.018827
21	6	0	-2.702682	-2.097707	2.822231
22	1	0	-3.455405	-2.650588	3.376682
23	6	0	-2.466198	0.170448	-1.663483
24	7	0	2.203910	-1.131411	0.080161
25	6	0	-2.070622	-0.979070	3.399339
26	1	0	-2.315583	-0.648022	4.402761
27	6	0	3.223388	-1.354089	0.944700
28	1	0	3.216850	-0.771277	1.860672
29	6	0	-4.906740	1.137346	-0.598485
30	6	0	-3.666911	-0.548400	-1.849677
31	1	0	-3.663348	-1.468265	-2.432941
32	6	0	-2.353632	-2.491329	1.518195
33	1	0	-2.829515	-3.347583	1.049858
34	6	0	-4.880619	-0.071664	-1.319069
35	1	0	-5.799558	-0.629294	-1.479950
36	6	0	-0.880620	-2.160561	-0.554236
37	1	0	-0.134123	-2.954404	-0.424003
38	1	0	-1.700888	-2.583446	-1.147078
39	6	0	2.144116	-1.828152	-1.086232
40	6	0	-3.715922	1.869617	-0.419376
41	1	0	-3.735107	2.814781	0.117131
42	6	0	-1.166945	-0.327197	-2.267938
43	1	0	-1.380759	-1.035582	-3.083525
44	1	0	-0.590699	0.508324	-2.676020
45	6	0	4.240195	-2.285725	0.674290
46	1	0	5.045075	-2.436043	1.386122
47	6	0	1.004903	-1.465706	-2.026175
48	1	0	1.319016	-0.619371	-2.647755
49	1	0	0.774654	-2.310549	-2.692688
50	6	0	-2.506584	1.390816	-0.951614
51	1	0	-1.597859	1.978722	-0.838397
52	6	0	4.183886	-3.012443	-0.530161
53	1	0	4.951034	-3.743371	-0.768740
54	6	0	3.118202	-2.785100	-1.421601
55	1	0	3.048442	-3.334711	-2.355889
56	1	0	-5.844231	1.512776	-0.196737

Table S3. List of coordinates for energy minimized structure of complex **2**

Center Number	Atomic Number	Atomic Type	Coordinates (Angstroms) X	Y	Z
1	6	0	7.040065	3.097812	0.964465
2	1	0	7.705044	2.406781	0.965010
3	1	0	6.984487	3.493571	1.836473
4	1	0	7.277768	3.771423	0.321420
5	8	0	-3.598042	0.932683	2.067600
6	8	0	-3.461063	-1.715940	1.113514
7	6	0	-4.213430	0.373280	3.023693
8	6	0	-4.516570	-1.000064	3.086523
9	1	0	-5.031370	-1.290244	3.805514
10	6	0	-4.642797	1.279675	4.119613
11	1	0	-4.359538	2.175958	3.924046
12	1	0	-4.244752	0.992314	4.945683
13	1	0	-5.598799	1.255678	4.199983
14	6	0	-4.112067	-1.946760	2.180183
15	6	0	-4.450887	-3.403752	2.395690
16	1	0	-4.090674	-3.926691	1.675263
17	1	0	-5.403686	-3.511676	2.423408
18	1	0	-4.070678	-3.700391	3.226299
19	29	0	-3.201635	0.058601	0.413810
20	7	0	-2.849670	-0.725115	-1.457596
21	6	0	-1.994799	1.603864	-1.617238
22	7	0	-2.222297	1.630636	-0.286341
23	6	0	-1.776948	2.673528	0.435698
24	1	0	-1.934646	2.693736	1.353195
25	6	0	-0.834818	3.686191	-1.485883
26	1	0	-0.361546	4.376111	-1.889825
27	9	0	7.500422	0.347143	-0.746243
28	6	0	-0.360658	-1.161451	-1.130103
29	7	0	-5.247600	0.134053	-0.457163
30	9	0	7.348831	0.086532	1.497848
31	6	0	-1.087733	3.712928	-0.152465
32	1	0	-0.797549	4.431623	0.361149
33	6	0	4.168021	1.000261	0.092825
34	6	0	-6.353867	0.751426	-0.053737
35	1	0	-6.307917	1.328244	0.674290
36	6	0	2.239100	-0.476298	-0.435591
37	6	0	2.065672	2.596853	-0.075952
38	1	0	1.585649	1.793278	-0.288254
39	1	0	1.988253	3.217743	-0.804939
40	1	0	1.694674	2.989886	0.718130
41	6	0	0.499043	-0.622191	-2.074724
42	1	0	0.202359	-0.495904	-2.947817
43	6	0	-1.299290	2.596598	-2.243963
44	1	0	-1.134129	2.554379	-3.158048
45	6	0	1.795613	-0.269716	-1.735690
46	1	0	2.362219	0.100949	-2.371628
47	6	0	-2.627270	0.446668	-2.339777
48	1	0	-3.477635	0.731095	-2.709367
49	1	0	-2.056188	0.182639	-3.077090
50	6	0	4.533759	-1.401418	-0.098804
51	6	0	4.299451	-2.773632	-0.319651
52	6	0	-5.327243	-0.706138	-1.503865
53	6	0	6.489778	-2.456996	-0.020017
54	6	0	5.535513	-3.372527	-0.257089
55	1	0	5.688476	-4.283654	-0.367426
56	7	0	5.532177	1.203226	0.377351
57	7	0	5.915731	-1.209971	0.099932
58	6	0	1.362096	-0.973590	0.518313
59	1	0	1.648684	-1.076383	1.396440
60	6	0	3.691642	-0.255653	-0.118854

61	5	0	6.618471	0.123183	0.325751
62	6	0	-1.711969	-1.703398	-1.526382
63	1	0	-1.652224	-2.040375	-2.432939
64	1	0	-1.919550	-2.456453	-0.948311
65	6	0	3.529079	2.269671	0.155825
66	6	0	-7.564161	0.567521	-0.675583
67	1	0	-8.324524	1.008332	-0.373285
68	6	0	-4.073704	-1.451063	-1.856800
69	1	0	-4.085919	-2.315924	-1.420181
70	1	0	-4.053824	-1.602155	-2.814475
71	6	0	0.084740	-1.311916	0.181245
72	1	0	-0.491956	-1.645610	0.828770
73	6	0	-7.629852	-0.276321	-1.744679
74	1	0	-8.442896	-0.427478	-2.166580
75	6	0	2.994928	-3.503025	-0.532667
76	1	0	2.267640	-2.875899	-0.493304
77	1	0	2.882842	-4.165869	0.153026
78	1	0	3.003020	-3.928371	-1.393061
79	6	0	7.976205	-2.642688	0.123341
80	1	0	8.390678	-1.791770	0.283053
81	1	0	8.329416	-3.024128	-0.684465
82	1	0	8.156517	-3.229958	0.861163
83	6	0	-6.502043	-0.901840	-2.196887
84	1	0	-6.527170	-1.444675	-2.951665
85	6	0	4.486573	3.184987	0.480236
86	1	0	4.352946	4.096953	0.600534
87	6	0	5.710945	2.510966	0.599407

Table S4. List of coordinates for energy minimized structure of complex **3**

Center Number	Atomic Number	Atomic Type	Coordinates (Angstroms) X	Y	Z
1	6	0	5.198400	4.071868	0.629689
2	1	0	5.797320	3.603904	1.417091
3	1	0	4.908903	5.078690	0.940628
4	1	0	5.843237	4.151968	-0.255473
5	8	0	-4.471044	0.218856	2.252038
6	8	0	-4.263501	-2.403033	1.209861
7	6	0	-4.578770	-0.419113	3.395457
8	6	0	-4.575028	-1.826490	3.532365
9	1	0	-4.682956	-2.231100	4.530931
10	6	0	-4.700664	0.464558	4.618893
11	1	0	-5.532307	1.167814	4.488225
12	1	0	-3.786514	1.061708	4.733901
13	1	0	-4.859688	-0.114801	5.531566
14	6	0	-4.415049	-2.744217	2.470670
15	6	0	-4.399335	-4.233049	2.745193
16	1	0	-3.452280	-4.665743	2.398226
17	1	0	-5.204364	-4.720464	2.180491
18	1	0	-4.524102	-4.457273	3.807223
19	29	0	-4.332759	-0.585343	0.463936
20	7	0	-3.956564	-1.373290	-1.475454
21	6	0	-3.582327	1.108762	-1.730258
22	7	0	-3.786376	1.155647	-0.388699
23	6	0	-3.633942	2.319258	0.295813
24	1	0	-3.818443	2.262516	1.362572
25	6	0	-3.044317	3.471456	-1.746215
26	1	0	-2.752581	4.372370	-2.277957
27	9	0	6.317286	1.448241	-0.562489
28	6	0	-1.402506	-1.580879	-1.194747
29	7	0	-6.427278	-0.689068	-0.340017

30	9	0	5.829177	1.170780	1.707288
31	6	0	-3.266663	3.504119	-0.355346
32	1	0	-3.154080	4.421235	0.212541
33	6	0	2.751889	1.390430	-0.109626
34	6	0	-7.560192	-0.074428	0.077573
35	1	0	-7.465571	0.582074	0.937073
36	6	0	1.169343	-0.508959	-0.609688
37	6	0	0.386275	2.521791	-0.503786
38	1	0	-0.198555	2.053422	0.298039
39	1	0	0.163365	1.979105	-1.428796
40	1	0	0.030744	3.550063	-0.618201
41	6	0	-0.486506	-1.290295	-2.228594
42	1	0	-0.745633	-1.514357	-3.262238
43	6	0	-3.201055	2.259693	-2.440898
44	1	0	-3.034897	2.208422	-3.512946
45	6	0	0.784113	-0.759118	-1.942018
46	1	0	1.483948	-0.560739	-2.749335
47	6	0	-3.857984	-0.212509	-2.428281
48	1	0	-4.811988	-0.118994	-2.962916
49	1	0	-3.087662	-0.401995	-3.185673
50	6	0	3.615645	-0.909274	-0.182610
51	6	0	3.685612	-2.349518	-0.314719
52	6	0	-6.468391	-1.523734	-1.412700
53	6	0	5.781973	-1.495402	0.159499
54	6	0	5.033772	-2.686614	-0.104169
55	7	0	4.039640	1.884868	0.202630
56	7	0	4.920105	-0.441495	0.111570
57	6	0	0.251302	-0.782665	0.427214
58	1	0	0.541778	-0.604480	1.459209
59	6	0	2.544192	0.002736	-0.293867
60	5	0	5.304614	1.025490	0.370346
61	6	0	-2.722542	-2.266722	-1.498999
62	1	0	-2.670694	-2.743469	-2.490430
63	1	0	-2.915951	-3.042937	-0.752981
64	6	0	1.857355	2.518948	-0.192169
65	6	0	-8.795929	-0.275344	-0.561112
66	1	0	-9.685498	0.228222	-0.197557
67	6	0	-5.166413	-2.226532	-1.762759
68	1	0	-5.073294	-3.120717	-1.136025
69	1	0	-5.174799	-2.547238	-2.815187
70	6	0	-1.014897	-1.316154	0.138530
71	1	0	-1.688842	-1.564783	0.955247
72	6	0	-8.845936	-1.135769	-1.674148
73	1	0	-9.783694	-1.310205	-2.193582
74	6	0	2.572702	-3.317078	-0.614809
75	1	0	2.228882	-3.226962	-1.653125
76	1	0	1.703952	-3.155837	0.031747
77	1	0	2.916533	-4.345646	-0.470575
78	6	0	7.240853	-1.334052	0.442534
79	1	0	7.392038	-0.738244	1.349476
80	1	0	7.730567	-0.790879	-0.375647
81	1	0	7.723409	-2.306385	0.561283
82	6	0	-7.664718	-1.765891	-2.110395
83	1	0	-7.675146	-2.432904	-2.967524
84	6	0	2.645386	3.652551	0.079923
85	6	0	3.992725	3.242801	0.320515
86	53	0	5.871508	-4.618122	-0.163639
87	53	0	1.990814	5.656174	0.127876

Table S5. Chemical structures of reference complexes mentioned in MTT assay in **Table 3**

Entry	Complex	Structure
1	**BODIPY-Pt** **(Ref. 57)**	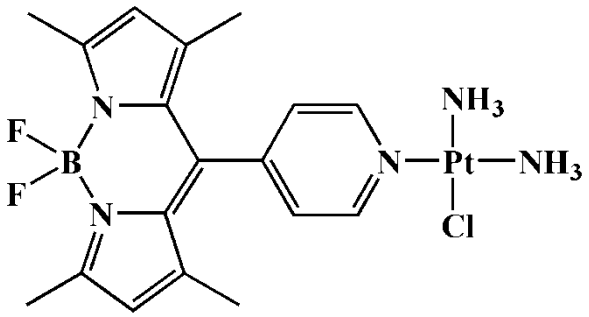
2	**[Ir-(BODIPY)-(ppy)]PF_6** **(Ref. 58)**	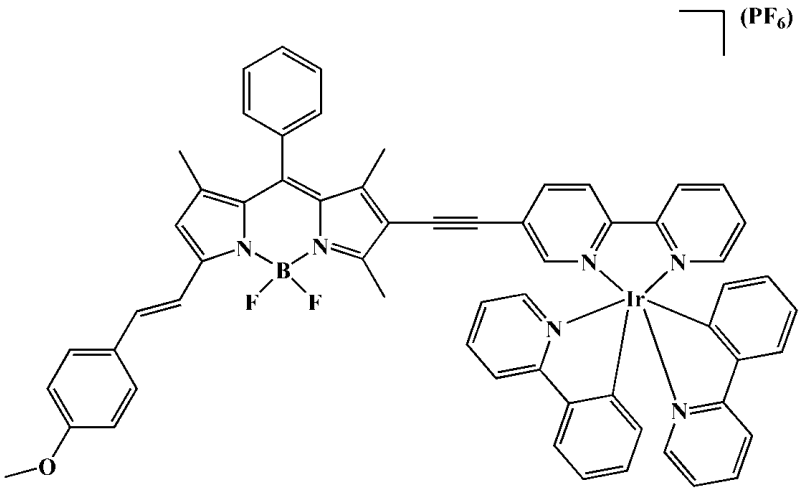

3	**[Cu-(BODIPY)-(curcumin)]Cl** **(Ref. 41)**	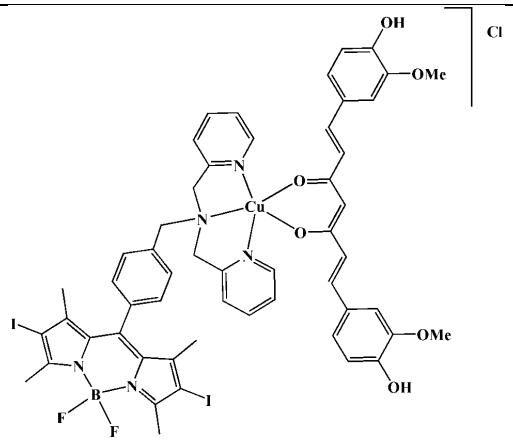
4	**[VO-(BODIPY)-(curcumin)]Cl** **(Ref. 59)**	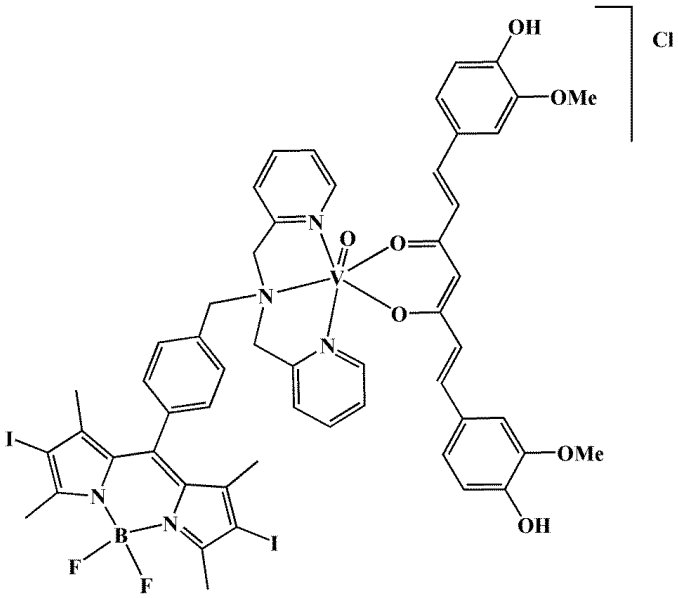

5	**[Cu(bba)-(5,6dmp)]$(ClO_4)_2$** **(Ref. 56a)**	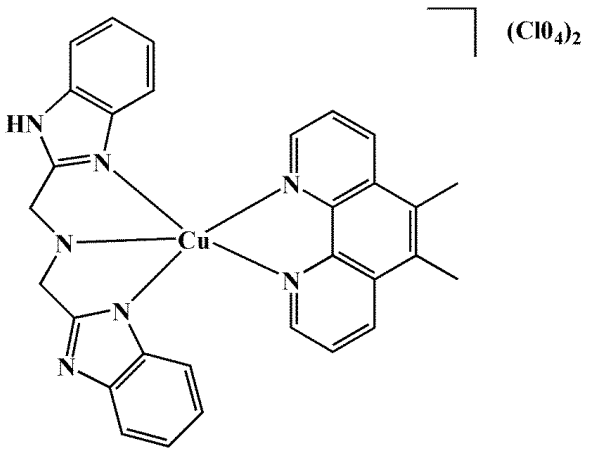
6	**[Cu-(pbt)-(Br_2)-(DMF)]** **(Ref. 56b)**